Project

Wake Turbulence Reclassification and Separation with Induced Power Using the FAA Aircraft Characteristics Database

Author: Marten Grunze

Supervisor: Prof. Dr.-Ing. Dieter Scholz, MSME
Submitted: 2025-06-30

Faculty of Engineering and Computer Science
Department of Automotive and Aeronautical Engineering

DOI:
https://doi.org/10.15488/xxxxx

URN:
https://nbn-resolving.org/urn:nbn:de:gbv:18302-aero2025-06-30.01
Associated URLs:
https://nbn-resolving.org/html/urn:nbn:de:gbv:18302-aero2025-06-30.01

Any further request may be directed to:
Prof. Dr.-Ing. Dieter Scholz, MSME
E-Mail see: http://www.ProfScholz.de

This work is part of:
Digital Library - Projects & Theses - Prof. Dr. Scholz
http://library.ProfScholz.de

Published by
Aircraft Design and Systems Group (AERO)
Department of Automotive and Aeronautical Engineering
Hamburg University of Applied Science

This report is deposited and archived:
- Deutsche Nationalbiliothek (https://www.dnb.de)
- Repository of Leibniz University Hannover (https://www.repo.uni-hannover.de)
- Internet Archive (https://archive.org)
  Item: https://archive.org/details/TextGrunze.pdf

This report has associated published data in Harvard Dataverse:
https://doi.org/10.7910/DVN/4YIYLN

Abstract

Purpose – The aim of this study is to reassess wake turbulence categorization (WTC) based on induced power and to link to established separation minima. The calculation of induced power requires these parameters: aircraft mass, wingspan, approach speed, air density, and the Oswald factor — which itself is calculated from wing aspect ratio, sweep angle, taper ratio, winglet height, and fuselage diameter. This approach is significantly more detailed than other metrics that consider only aircraft mass or a combination of mass and wingspan.

Methodology – In a previous classification, 89 aircraft types were grouped only into four categories based on their calculated induced power. With the FAA Aircraft Characteristics Database, the necessary parameters for calculating induced power are accessible for 388 aircraft, which were grouped into six categories. This broader dataset allows for a refined statistical analysis and better comparison with other classification systems, enabling the definition of new category thresholds for an own WTC (called HAW WTC) based on induced power. Additionally, a continuous separation formula was developed.

Findings – The simple calculation of induced power (the product of induced drag and aircraft speed) is the same as the energy of the vortex shed from the wing per time. WTC separation minima got proposed following EUROCONTROL, but now with physics-based WTCs from induced power. Continuous (non-classifying) separation minima can be calculated with a new equation. Its structure is conceived from non-linear regression. Input parameters are induced power of leader and follower aircraft as well as the difference of their induced power. Five regression parameters were optimized with Excel's Solver based on EUROCONTROL and ICAO separation minima.

Research Limitations – Aircraft responses of the following aircraft are only envisioned from flying behind and parallel to the leading aircraft and directly through the vortex core. It is assumed that the resistance to roll of the following aircraft is related to its induced power. This seems plausible, but no proof is given. The analysis is statistical only. Other dangers like intersecting vortices at an angle are not considered.

Practical Implications – Separation minima can easily be obtained from a table based on six physics-based wake turbulence categories. Pairwise separation minima for specific leader and follower aircraft can be calculated without categorization boundaries. These dedicated separation minima have the potential to improve efficiency and safety for aircraft on approach. In the next step it is necessary to discuss data handling at Air Traffic Control (ATC) units. It also needs an agreed graphical representation of the calculated pairwise separation minima suitable for controllers at work.

Originality – To use induced power as a metric for WTC was proposed by Scholz in 2022 and was subsequently applied by Camilo. This report provides further details with 388 aircraft investigated and an in-depth statistical analysis.

DEPARTMENT OF AUTOMOTIVE AND AERONAUTICAL ENGINEERING

Wake Turbulence Reclassification and Separation with Induced Power Using the FAA Aircraft Characteristics Database

Task for a *Project*

Background

Aircraft produce wake turbulence or wake vortex turbulence. The whole topic is covered here with many articles. Depending on their vortex strength, aircraft are put in Wake Turbulence Categories (WTC). The criteria for the categories vary. ICAO goes by aircraft mass and lists aircraft by category. EUROCONTROL goes by aircraft mass and wing span (Figure 6) and also lists aircraft by category (Table 2). Also, the FAA lists aircraft by category (Table A-1). Flight mechanics on the topic can be quite simple. The vortex strength can be calculated with what we call "induced power". I have explained it here. Camilo (2022) has written on "Comparing Aircraft Wake Turbulence Categories with Induced Power Calculation". With help of the FAA Aircraft Characteristics Database (ACD) refinement is possible of own WTCs.

Task

Your task is

- to describe the FAA Aircraft Characteristics Database (FAA ACD),
- to present established wake turbulence classifications by ICAO, Eurocontrol, FAA, and an initial induced power-based HAW WTC,
- to apply the parameters used for ICAO, FAA, and EU classifications to the aircraft types listed in the FAA ACD,
- to calculate induced power during approach based on Camilo (2022), using the available parameters from the FAA Aircraft Characteristics Database for all listed aircraft types,
- to develop a comparable induced power-based WTC, aligned with the category thresholds of RECAT-EU and RECAT-ICAO,
- to derive a formula-based, continuous aircraft separation model based on the separation charts from RECAT-EU and RECAT-ICAO,
- to apply the new formula to exemplary calculations of new separations, and to compare it with other separation charts.

The report has to be written in English based on German or international standards on report writing.

Table of Contents

List of Figures

List of Tables

List of Symbols

A	aspect ratio
b	wingspan
$C_{D,0}$	zero drag coefficient
C_L	lift coefficient
C_{D_i}	induced drag
d_F	fuselage diameter
E_k	kinetic energy per unit length
e_{theo}	theoretical Oswald factor
e	Oswald factor
g	gravitational acceleration
h	winglet height
$k_{e,D0}$	correction factor (viscous drag)
$k_{e,F}$	correction factor (fuselage)
$k_{e,M}$	correction factor (compressibility)
$k_{e,WL}$	correction factor (winglets)
L	lift force
m	aircraft mass
M	Mach-Number
P_{wake}	induced power
r_c	vortex core radius
S	wing area
V	airspeed

Greek Symbols

Δ	Difference
φ25	quarter chord sweep
Γ_v	circulation
λ	taper ratio
ρ	air density

List of Abbreviations

ACD	Aircraft Characteristics Database
ADG	Airplane Design Group
AVOSS	Aircraft Vortex Spacing System
BADA	Base of Aircraft Data
CAA	Civil Aviation Authority
CWT	Certified Weight Classification
FAA	Federal Aviation Administration
HAW	Hochschule für Angewandte Wissenschaften Hamburg (Hamburg University of Applied Sciences)
ICAO	International Civil Aviation Organization
LAHSO	Land and Hold Short Operations
MALW	Maximum Allowable Landing Weight
MTOW	Maximum Takeoff Weight
MW	Megawatt
NAS	National Airspace System
OEW	Operational Empty Weight
SRS	Standard Runway Separation
TDG	Taxiway Design Group
TMFS	Traffic Management Facilities
US	United States
WTC	Wake Turbulence Category

1 Introduction

1.1 Motivation

One of the main challenges aviation will face in the coming years is the rising number of passengers and, consequently, the increasing volume of aircraft operations. Both airspace and, more critically, airport capacities are limited. At the same time, aircraft must maintain a minimum separation to avoid encountering wake vortices generated by preceding aircraft that, in the worst case, could pose a threat to flight safety. Since wake vortices are an unavoidable consequence of lift generation, they must always be taken into account.

The key challenge lies in assigning aircraft to wake turbulence categories as precisely as possible to allow for the highest feasible number of flight operations, while ensuring that safety remains the top priority. The number of categories and the criteria used for classification vary among aviation authorities, but aircraft mass and wingspan are typically the primary factors for categorization.

As an alternative to traditional classification methods, this approach incorporates individual aircraft parameters to calculate induced power. Based on these calculations, new, potentially more accurate wake turbulence classification can be developed. With such reassessment, it may be possible to optimize minimum separation standards and increase airport capacities. This thesis therefore aims to reevaluate the current wake turbulence categorization system and explore the feasibility of transitioning from rigid, discrete categories to a function-based, continuous approach to aircraft separation.

1.2 Title Terminology

The title of this thesis is “Wake Turbulence Reclassification and Separation with Induced Power Using the FAA Aircraft Characteristics Database”. Following is a definition of each of the terms found in the title.

Wake Turbulence
Skybrary (2025) defines Wake […] Turbulence as:

> *turbulence which is generated by the passage of an aircraft in flight*

Reclassification
Cambridge Dictionary (2025a) defines reclassification as:

> *the act or process of dividing things into new or different groups according to their type*

Separation
Cambridge Dictionary (2025b) defines separation as:

> *the act of separating two or more people or things, or the state of being separated*

Induced Power
In Scholz (2022) the term induced power is defined as:

> *The power an aircraft continually contributes to its wake vortex*

Using
Present participle of use. Cambridge (2025c) defines use as:

> *to put something such as a tool, skill, or building to a particular purpose*

FAA
Abbreviation for Federal Aviation Administration. Cambridge (2025d) defines the Federal Aviation Administration as:

> *a US government organization that makes the rules relating to planes and airports in the US and makes sure that these rules are obeyed*

Aircraft
Longman (2025a) defines Aircraft as:

> *a plane or other vehicle that can fly*

Characteristics
Longman (2025b) defines characteristics as:

> *a quality or feature of something or someone that is typical of them and easy to recognize*

Database
Longman (2025c) defines database as:

> *a large amount of data stored in a computer system so that you can find and use it easily*

1.3 Objectives

The objective of this thesis is to reassess the HAW WTC, based on induced power calculation. To achieve this, the induced power of 388 aircraft listed in the FAA Aircraft Characteristics Database will be calculated, providing a broad spectrum of aircraft types in terms of mass, wingspan, and other relevant characteristics. Based on the outcomes of these calculations, new wake turbulence categories will be proposed and compared to established categorization systems currently used by ICAO and Eurocontrol. Furthermore, a novel approach separation minima formula will be developed to enable a function-based and continuous separation concept, moving away from rigid, discrete category boundaries.

1.4 Literature Review

The foundation of this thesis is the FAA Aircraft Characteristics Database (FAA 2025a), which provides most of the technical data for the aircraft examined and used in the calculations.

The thesis written by Camilo (2022) offers a comprehensive overview of wake vortex generation, wake encounter scenarios, the parameters influencing such encounters, and the different phases of vortex evolution. In addition, Camilo (2022) introduced an initial approach for calculating induced power, drawing on several references that are also used in this thesis.

The equation used for the induced power calculation is derived from Scholz (2022), while the methods and formulas for estimating the Oswald efficiency factor are based on Nita (2012). Furthermore, existing wake turbulence categorization systems defined by Eurocontrol (2024) and ICAO (2021) serve as reference points for comparison with the proposed categorization based on induced power, particularly in relation to approach separation minima.

1.5 Structure of the Work

This thesis is structured into nine chapters, each covering the following content:

Chapter 2 provides a review of an existing induced power calculation method and current separation schemes used for wake vortex separation.

Chapter 3 describes the FAA Aircraft Characteristics Database, which serves as the primary source of aircraft data used in this thesis.

Chapter 4 explains the theoretical basics of wake turbulence and presents existing aircraft wake turbulence classification systems currently used by international aviation authorities and an induced power WTC.

Chapter 5 explains the methodology for the calculation of induced power.

Chapter 6 presents the results of the induced power calculations and compares them with conventional classification systems.

Chapter 7 introduces a methodology to determine continuous approach separation minima based on induced power.

2 State of the Art

The foundation of this project is the master thesis by Camilo (2022). That work investigates and collects the theoretical principles of wake turbulence described in Breitsamter (2010) and Anderson (1999), including how wake vortices are generated, the conditions under which wake encounters occur, presented in De Kat (2007), and the factors influencing both vortex behavior and wake-related risks. Additionally, it offers a comprehensive overview of existing wake turbulence classification systems and various vortex models. A central component of Camilo (2022) is the calculation of induced power for a total of 87 aircraft models. These calculations are based on the induced power equation derived by Scholz (2022) and the methodology for estimating the Oswald factor proposed by Nita (2012). These three references also form the methodological foundation for the calculations carried out in this thesis. As part of the induced power analysis, Camilo (2022) presents an initial attempt at classifying aircraft into Wake Turbulence Categories, using the ICAO categorization as a reference framework. This classification is then compared with other established systems from the FAA, CAA, Eurocontrol, and ICAO.

Over time, almost every major aviation authority has developed its own categorization scheme. The primary goal of this aircraft WTC categorization is minimizing wake-related risks and supporting the coordination of arrivals and departures to ensure operational safety at airports. The most widely used and recognized classification systems, namely those of ICAO (2021), Eurocontrol (2024), and FAA (2021), are predominantly based on maximum takeoff weight but may also incorporate aircraft wingspan and approach speed. A review of recent developments and reclassification efforts by the aviation authorities reveals a clear trend toward an increasing number of more finely subdivided categories. Based on these classifications, authorities issue recommended aircraft separation standards for both approach and departure. The corresponding separation charts are well established and contribute to maintaining flight safety, serving at the same time as a foundation for future separation concepts.

Nevertheless, existing classifications share a common limitation: aircraft are assigned to fixed and discrete categories by only two parameters, MTOW and wingspan, offering no flexibility to account for operational parameters that vary in flight, such as aircraft mass, approach speed, or other performance-related variables. As of now, there is no classification model that enables a continuous and dynamic assessment of wake turbulence risk. To build upon and extend the work of Camilo (2022), this project uses the FAA (2025a) Aircraft Characteristics Database as its primary data source. The database contains essential performance and operational parameters for 388 aircraft models and, due to its broad and representative coverage, enables a good statistical analysis. This serves as the foundation for developing a continuous classification approach and allows for a comparative evaluation against existing categorization systems.

3 The FAA Aircraft Characteristics Database

3.1 Introduction

The FAA Aircraft Characteristics Database (ACD), by FAA (2025a), serves as a comprehensive repository of aircraft specifications used throughout the National Airspace System (NAS). It provides critical data for airport planning, air traffic management, aircraft performance analysis, and regulatory compliance. Additionally, it is a valuable resource for studies and calculations involving approach speeds, physical dimensions, weight classifications, and wake turbulence characteristics.

The database contains entries for 388 aircraft models from 90 different manufacturers, such as Airbus, Boeing, Embraer, Canadair, Pilatus, and Cessna. As illustrated in Figure 3.1, the database includes a wide variety of propulsion systems across different aircraft types. Moreover, models of all FAA weight classes are represented in the database, as shown in Figure 3.2. These range from “Small” aircraft with a maximum takeoff weight (MTOW) of less than 12,500 lb to the “Super” category, which in this database is exclusively assigned to the Airbus A380-800.

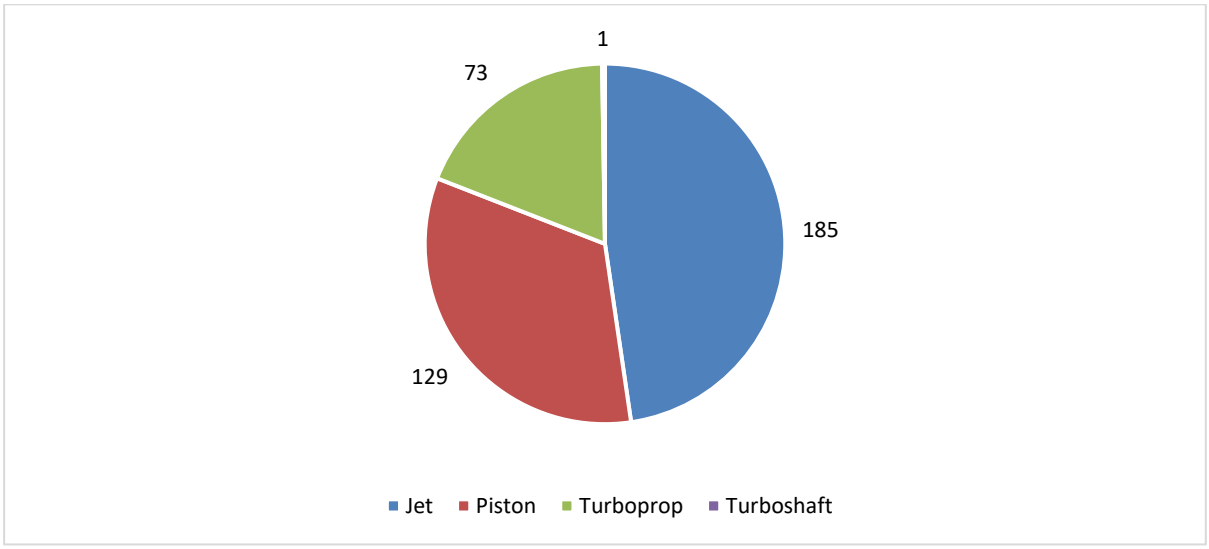

Figure 3.1 Number of Aircraft Models per Engine Type

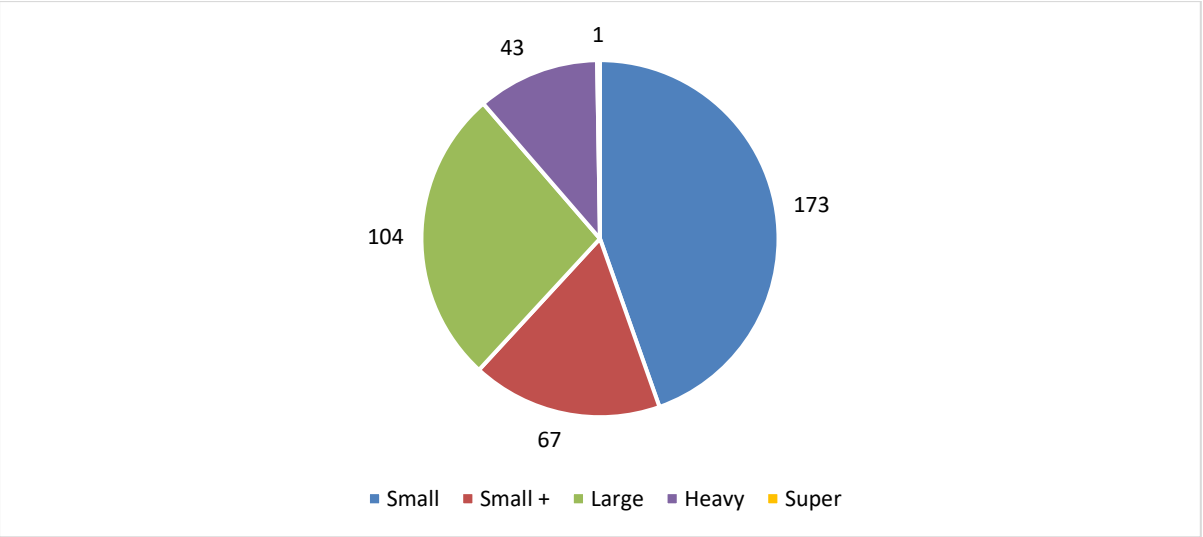

Figure 3.2 Number of Aircraft Models per FAA Weight Class

3.2 Structure and Content

The FAA Aircraft Characteristics Database consists of multiple datasets, with the ACD data table comprising 388 aircraft entries and 56 attributes. These attributes can be organized in categories as follows.

Aircraft Identification and Classification
To ensure global standardization and consistent identification across aviation systems, each aircraft model is associated with standardized identifiers. These include the ICAO aircraft type designator used in flight plans and air traffic control communication, as well as the FAA designator used within U.S. airspace. The database also records the aircraft manufacturer, the FAA-recognized model name, and the BADA designation used in Eurocontrol's performance models.

Aircraft Dimensions and Physical Properties
The dataset includes key dimensional values such as wingspan (with and without winglets), aircraft length, tail height, and landing gear configuration. These parameters are essential for infrastructure planning, aircraft maneuverability assessments, and determining spatial requirements for taxiways, gates, and parking stands. Each aircraft is also categorized by type, distinguishing between fixed-wing and tiltrotor models.

Weight and Performance Characteristics
Weight and performance characteristics are fundamental for operational planning and airport infrastructure design. The database provides values such as Maximum Takeoff Weight (MTOW) and Maximum Landing Weight (MALW), which are critical for runway strength

assessment and fuel calculations. Additional attributes include propulsion type, number of engines, and parking area size. Certified Weight Classifications (CWT) are also included, serving as a basis for air traffic management decisions and airport fee structures.

Approach Speed and Wake Turbulence Classification

Approach speeds and wake turbulence profiles significantly impact runway occupancy times and separation standards. The database includes each aircraft's standard approach speed as well as its Aircraft Approach Category (AAC), which defines minimum runway length requirements based on speed. Multiple wake turbulence categories are recorded, including the ICAO Wake Turbulence Category (WTC) and additional classifications used in specific ATC procedures.

Operational Requirements and Restrictions

To support airport layout and airspace management, the database contains operational classifications such as FAA Weight, Airplane Design Group (ADG), and Taxiway Design Group (TDG), all of which are based on aircraft dimensions and gear configurations. Additional parameters such as main gear configuration, standard runway separation (SRS), and Land and Hold Short Operations (LAHSO) distances are included to ensure safe and efficient ground operations. For rotary-wing aircraft, rotor diameter is provided to support heliport and mixed-use airfield planning.

FAA Registry and Traffic Data

The database also incorporates registry and operational data from the FAA. It indicates whether an aircraft model is registered, provides the number of active registrations, and records the total number of operations per aircraft type for fiscal year 2024 (TMFS_Operations_FY24). This information supports analysis of aircraft usage trends and operational demand within U.S. airspace.

4 Wake Turbulence and Classifications

4.1 Physics of Wake Turbulence and its Influencing Factors

As described in Breitsamter (2010), wake turbulence is an inevitable result of lift generation by a wing. Lift arises due to a pressure difference between the upper and lower surfaces of the wing, caused by differing airflow velocities. The air on the upper surface accelerates more than the air on the lower surface, leading to lower pressure above the wing in accordance with Bernoulli's principle. Because the wing has a finite span, the resulting pressure imbalance causes airflow to curve around the wingtips, forming concentrated rotational flows known as wing tip vortices. The region between these two counter-rotating vortices is characterized by a downward-directed induced flow, commonly referred to as downwash. Depending on environmental conditions, these vortices can persist for several minutes, gradually descending and spreading laterally, while atmospheric turbulence and instabilities contribute to their eventual dissipation. The structure and behavior of wake vortices are illustrated in Figure 4.1 and Figure 4.2.

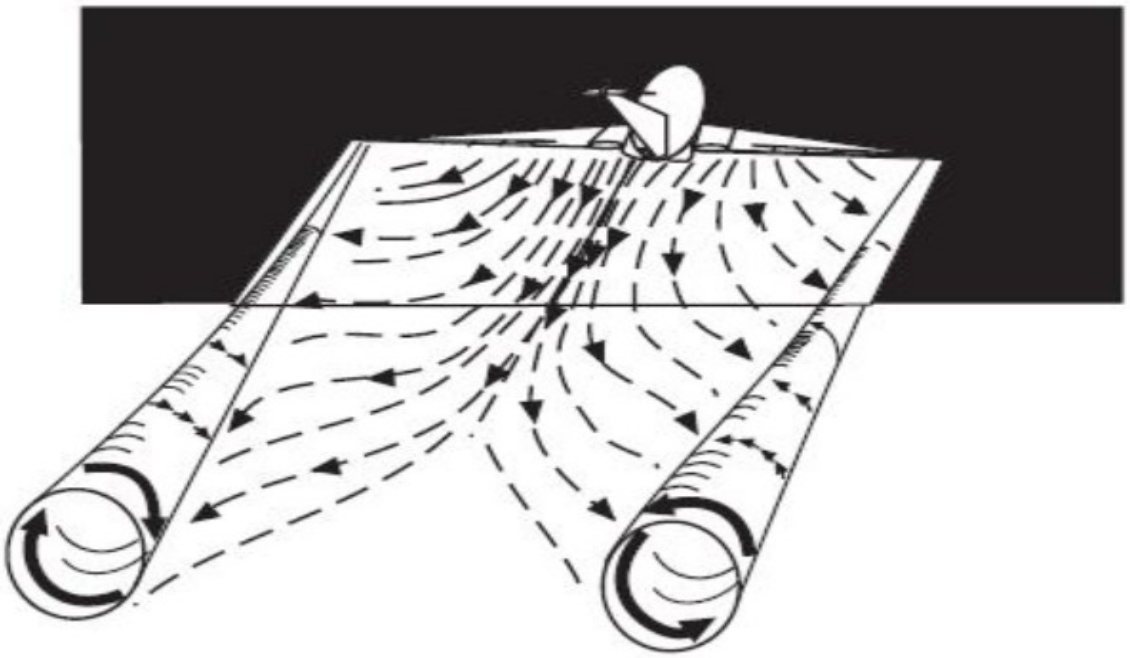

Figure 4.1 Schematic of Wake Turbulence Formation (FAA 2025b)

Figure 4.2 Formation of Wake Vortices Behind an Aircraft (Ewing 2025)

According to Breitsamter (2010), the wake of an aircraft can be divided into four distinct regions. In the near field, highly concentrated vortices form immediately behind the wings. This is followed by the extended near field, in which the vortex roll-up process begins and individual co-vortices merge into two dominant counter-rotating structures. In the mid and far field, the vortices continue to descend and gradually decay under the influence of atmospheric conditions. Finally, in the decay or dispersion region, the vortices break down completely due to ambient turbulence and flow instabilities. These stages are schematically represented in Figure 4.3.

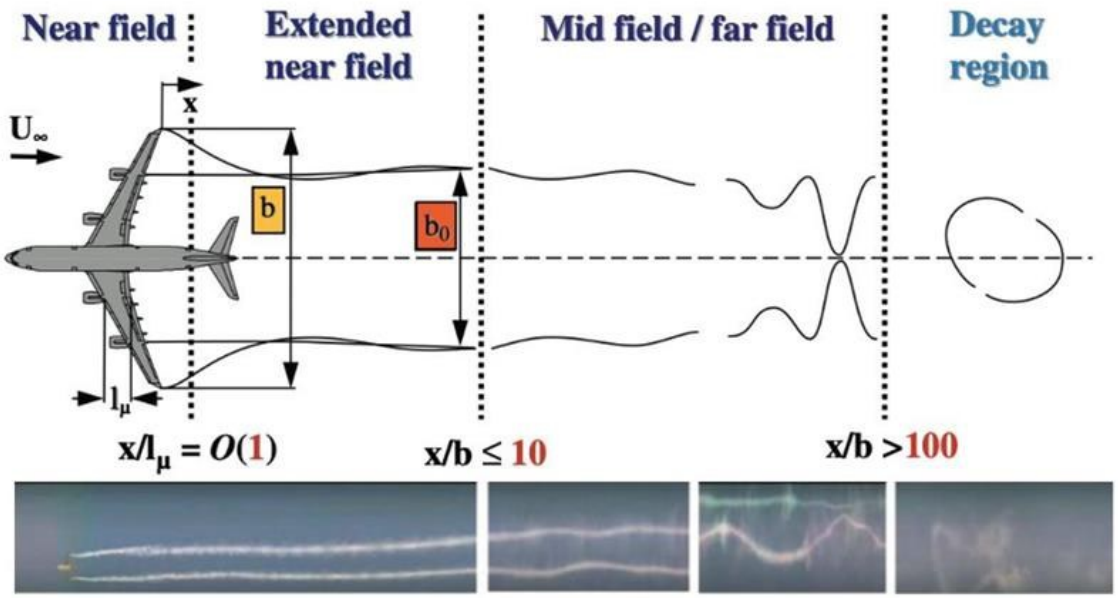

Figure 4.3 Schematic of Four Stages of an Aircraft Wake (Breitsamter 2010)

Several factors influence the effect of wake vortices on trailing aircraft, as shown in Camilo (2022). The generation and roll-up of wake vortices are primarily governed by the

characteristics of the leading aircraft, including its weight, wingspan, spanwise lift distribution, and stall speed. Flight parameters such as velocity and ambient air density also influence the aircraft roll-up. In addition, meteorological conditions, such as wind speed and direction, turbulence intensity, and temperature gradients, affect vortex aging and persistence. For example, low wind speeds and stable stratification can prolong the vortex lifetime significantly. Ultimately, the impact on a following aircraft is determined not only by the properties of the aged wake vortex, but also by the aerodynamic configuration of the trailing aircraft, such as its speed, wingspan, aspect ratio, taper ratio, and its relative position to the vortex core in both, vertical and horizontal directions (Figure 4.4).

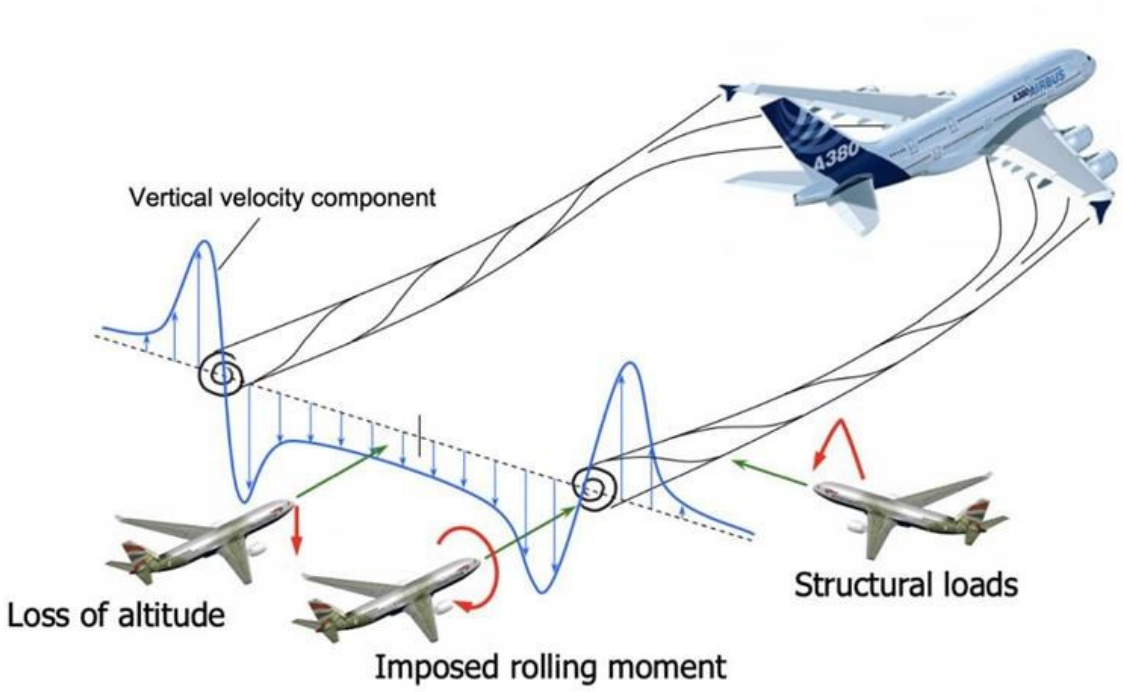

Figure 4.4 Three Typical Scenarios of Wake Vortex Encounters (De Kat 2007)

As described in De Kat (2007), three different scenarios, as shown in Figure 4.4 for vortex encounters are the most typical.

Scenario 1: The trailing aircraft intersects the vortex field perpendicularly. This can lead to high structural loads and intense turbulence, potentially resulting in significant dynamic response of the aircraft.

Scenario 2: The aircraft flies parallel to and between the two counter-rotating vortices. The downwash in this region may reduce the aircraft's climb rate or increase its rate of descent, posing a substantial risk during final approach.

Scenario 3: The aircraft flies along the vortex axis. This scenario is considered particularly hazardous, as the aircraft enters a velocity field that can induce a strong rolling moment. This

is especially critical at low altitudes, such as during final approach, where the aircraft's roll control authority may not be sufficient to counteract the disturbance.

The investigation in this thesis is limited to Scenario 2, in which all aircraft are assumed to follow an identical glide path during the approach phase and are positioned centrally between the wake vortices generated by the preceding aircraft. Influences from external factors such as meteorological conditions or air traffic management procedures are deliberately excluded from the analysis. It is further assumed that these vortices are not displaced onto the glide path of the following aircraft by wind or other environmental effects, which would otherwise result in Scenario 3 and require a different analytical treatment.

4.2 Eurocontrol WTC RECAT-EU

The European Organization for the Safety of Air Navigation (EUROCONTROL) has introduced a revised version of the first ICAO wake turbulence categorization, known as "RECAT-EU," as presented in EUROCONTROL (2024). Unlike the first ICAO classification, which was primarily based on aircraft mass, the RECAT-EU framework also incorporates wingspan as a key parameter. The primary objective of this re-categorization is to enhance airport capacity by optimizing wake turbulence categories and separation minima, while maintaining established safety standards.

As shown in Figure 4.5, Eurocontrol classifies aircraft in RECAT-EU into six categories, ranging from CAT-A to CAT-F, based on maximum certified take-off mass (MTOM) and wingspan. Aircraft with an MTOM of less than 15,000 kg are classified as CAT-F (Light). Those with a take-off mass up to 100,000 kg fall under the Medium category. Within this category, aircraft are further divided based on wingspan: if the wingspan is less than 32 m, they are assigned to CAT-E (Lower Medium); otherwise, if the wingspan exceeds 32 m, they are categorized as CAT-D (Upper Medium). Aircraft with an MTOM greater than 100,000 kg are classified as Heavy. If the wingspan is less than 52 m, the aircraft is placed in CAT-C (Lower Heavy). For wingspans between 60 m and 72 m, CAT-B (Upper Heavy) applies. Aircraft with wingspans greater than 72 m fall under CAT-A (Super Heavy). For wingspans in the range of 52 m to 60 m, the classification depends on a more detailed analysis, with assignment to either CAT-C or CAT-B. Due to the extensive number of aircraft in the database, those falling under the "Specific Analysis" category are conservatively assigned to CAT-B.

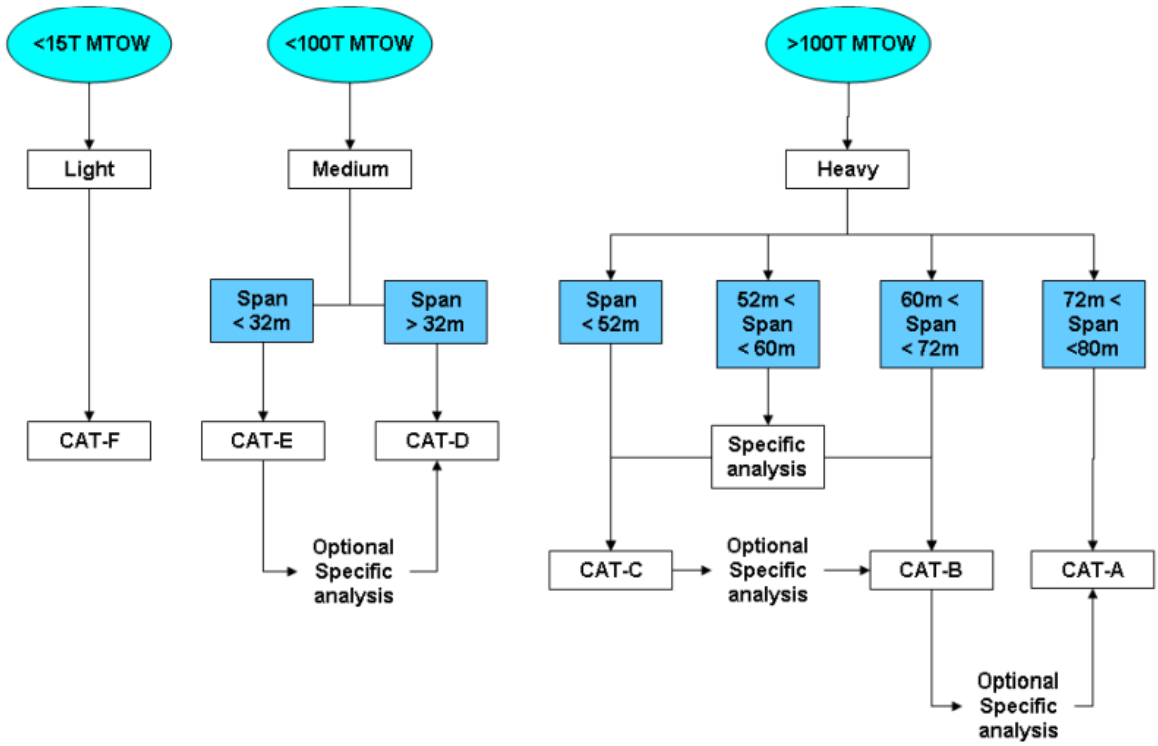

Figure 4.5 Wake Turbulence Categorization Scheme by Eurocontrol (Eurocontrol 2024)

Based on the categorisation made for each aircraft, as shown in Figure 4.5, separation minima are derived by Eurocontrol and presented in Figure 4.6.

RECAT-EU scheme		*"Super Heavy"*	*"Upper Heavy"*	*"Lower Heavy"*	*"Upper Medium"*	*"Lower Medium"*	*"Light"*
Leader / Follower		"A"	"B"	"C"	"D"	"E"	"F"
"Super Heavy"	"A"	**3 NM**	**4 NM**	**5 NM**	**5 NM**	**6 NM**	**8 NM**
"Upper Heavy"	"B"		**3 NM**	**4 NM**	**4 NM**	**5 NM**	**7 NM**
"Lower Heavy"	"C"		**(*)**	**3 NM**	**3 NM**	**4 NM**	**6 NM**
"Upper Medium"	"D"						**5 NM**
"Lower Medium"	"E"						**4 NM**
"Light"	"F"						**3 NM**

Figure 4.6 RECAT-EU WTC Distance-Based Separation Minima on Approach and Departure (Eurocontrol 2024)

4.3 ICAO WTC RECAT-ICAO

The ICAO transitioned from its original wake turbulence categorization based solely on maximum take-off weight (MTOW) to a classification like RECAT-EU, that considers both MTOW and wingspan. As of ICAO (2021), aircraft are now grouped into wake turbulence categories as follows.

GROUP A — aircraft types of 136,000 kg or more, and a wing span less than or equal to 80 m but greater than 74.68 m;
GROUP B — aircraft types of 136,000 kg or more, and a wing span less than or equal to 74.68 m but greater than 53.34 m;
GROUP C — aircraft types of 136,000 kg or more, and a wing span less than or equal to 53.34 m but greater than 38.1 m;
GROUP D — aircraft types less than 136,000 kg but more than 18,600 kg, and a wing span greater than 32 m;
GROUP E — aircraft types less than 136,000 kg but more than 18,600 kg, and a wing span less than or equal to 32 m but greater than 27.43 m;
GROUP F — aircraft types less than 136,000 kg but more than 18,600 kg, and a wing span less than or equal to 27.43 m;
GROUP G — aircraft types of 18,600 kg or less (without wing span criterion)

Variants of an aircraft type with different take-off masses might be classified within different wake turbulence categories. Civil aviation authorities of individual states may also make further changes to the classification and, for example, introduce additional categories. Based on the Aircraft Categories from the ICAO WTC, the ICAO implemented a new separation Chart for approaching and departing aircraft as in Table 4.1.

Table 4.1 ICAO Wake Turbulence Separation Minima (ICAO 2021)

Leader/ Follower	CAT B	CAT C	CAT D	CAT E	CAT F	CAT G
CAT A	4NM	5NM	5NM	6NM	6NM	8NM
CAT B	3NM	4NM	4NM	5NM	5NM	7NM
CAT C			3NM	3,5NM	3,5NM	6NM
CAT D						4NM
CAT E						4NM

4.4 FAA WTC RECAT

The Federal Aviation Administration classifies wake turbulence in FAA 2021 by using the following categories:

- Category A – A388 and A225
- Category B – Pairwise Upper Heavy aircraft
- Category C – Pairwise Lower Heavy aircraft
- Category D – Non-Pairwise Heavy aircraft
- Category E – B757 aircraft
- Category F – Upper Large aircraft excluding B757 aircraft
- Category G – Lower Large aircraft
- Category H – Upper Small aircraft with a maximum takeoff weight of more than 15,400 pounds up to 41,000 pounds
- Category I – Lower Small aircraft with a maximum takeoff weight of 15,400 pounds or less.

Based on the categorisation made for each aircraft, separation minima are derived by the FAA and presented in Figure 4.7.

A Super	B Upper Heavy	C Lower Heavy	D Non-Pairwise Heavy		E B757	F Upper Large		G Lower Large		H Upper Small	I Lower Small
A388	A332	A306	A124	DC85	B752	A318	C130	AT43	E170	ASTR	BE10
A225	A333	A30B	A339	DC86	B753	A319	C30J	AT72	E45X	B190	BE20
	A343	A310	A342	DC87		A320	CVLT	CL60	E75L	BE40	BE58
	A345	B762	A3ST	E3CF		A321	DC93	CRJ1	E75S	B350	BE99
	A346	B763	A400	E3TF		B712	DC95	CRJ2	F16	C560	C208
	A359	B764	A50	E6		B721	DH8D	CRJ7	F18H	C56X	C210
	B742	C17	AN22	E767		B722	E190	CRJ9	F18S	C680	C25A
	B744	DC10	B1	IL62		B732	GL5T	CRJX	F900	C750	C25B
	B748	K35R	B2	IL76		B733	GLEX	DC91	FA7X	CL30	C402
	B772	MD11	B52	IL86		B734	GLF5	DH8A	GLF2	E120	C441
	B773		B703	IL96		B735	GLF6	DH8B	GLF3	F2TH	C525
	B77L		B741	K35E		B736	MD82	DH8C	GLF4	FA50	C550
	B77W		B743	KE3		B737	MD83	E135	SB20	GALX	P180
	B788		B74D	L101		B738	MD87	E145	SF34	H25B	PAY2
	B789		B74R	MYA4		B739	MD88			LJ31	PA31
	C5		B74S	R135			MD90			LJ35	PC12
	C5M		B78X	T144						LJ45	SR22
			BLCF	T160						LJ55	SW3
			BSCA	TU95						LJ60	
			C135	VMT						SH36	
			C141							SW4	

Figure 4.7 Aircraft Types Assigned to Wake Turbulence Categories (FAA 2021)

Since the overview shown in Figure 4.7 is not based on a defined set of criteria for assigning all aircraft models in the FAA ACD, it cannot be used for evaluation or comparison with other Wake Turbulence Categories in the further course of this study.

4.5 HAW WTC

According to Scholz (2022), to generate wake vortices certain energy is required, which leads to the induced drag of the aircraft. The induced power is the induced drag multiplied with the aircraft speed and at the same time the power induced into the wake of an airplane while generating lift. Consequently, lots of lift implies lots of induced power put into an aircraft's wake vortex. According to Anderson (1999) “the power needed to lift the airplane is proportional to the load (or weight) times the vertical velocity of the air”. Furthermore, it can be concluded from the above-mentioned correlation that the required power for lift increases with higher mass. In the following, the equation for induced power is derived from induced drag (as a function of lift) and also from the energy in the vortex.

In a first approach, made in Camilo (2022), 89 different Aircraft models were selected and investigated for the calculation of induced power produced. To avoid complexity this approach was based on ICAO WTC and four different categories were defined. The Categorisation is shown in Table 4.2 and Results for Induced Power are shown in Figure 4.8.

Table 4.2 First HAW Hamburg Wake Turbulence Categories Based on Induced Power (Camilo 2022)

HAW Hamburg WTC	Induced Power [MW]
CAT I	> 15
CAT II	5 – 15
CAT III	1 – 5
CAT IV	< 1

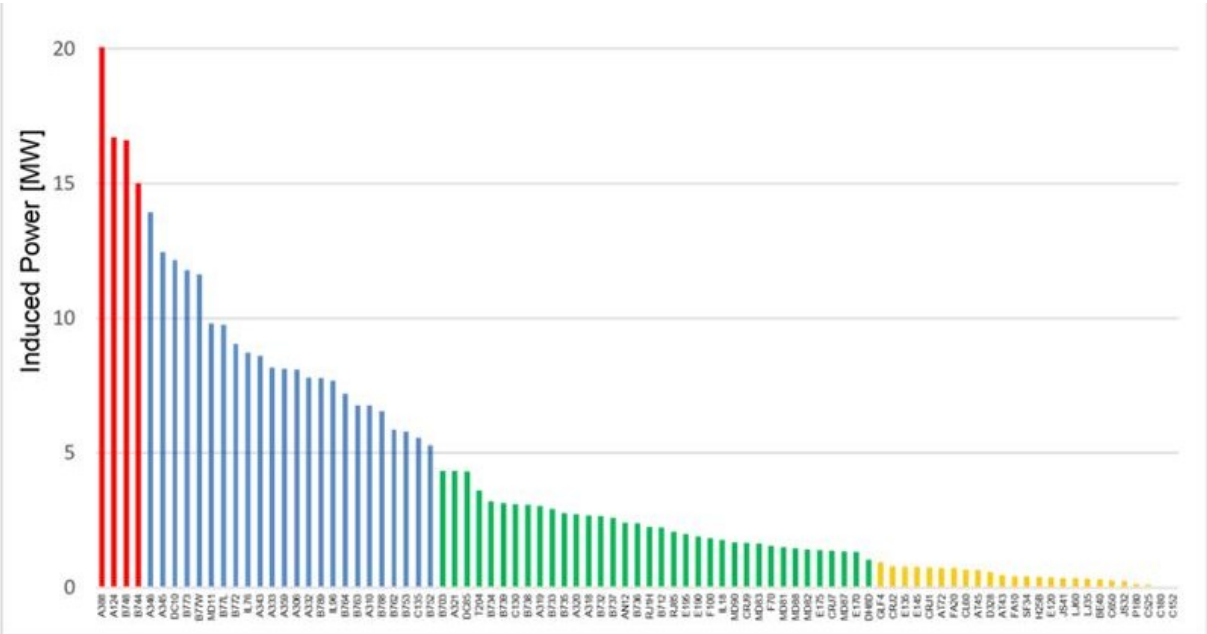

Figure 4.8 Examined Aircraft Sorted According to Induced Power in Descending Order (Camilo 2022)

5 Induced Power Methodology

As described by Scholz (2018), when an aircraft generates lift, the wing pushes the surrounding air downward. At the same time, the airflow near the wingtips moves upward and inward, while air behind the wing moves downward and outward. This interaction creates two vortices that rotate in opposite directions.

No matter which vortex model, explained in Camilo (2022), is applied, producing these wake vortices always requires a certain amount of energy. This energy is reflected in the aircraft's induced drag. Induced power refers to the portion of energy transferred into the wake as lift is generated. Therefore, higher lift demand leads to more energy being fed into the wake vortices.

5.1 From Overall Induced Power to the Power in the Vortex

The approach used in this paper to categorize wake vortex strength, considers the induced power contributed by the respective aircraft to its wake vortex.

According to Scholz (2022), the induced power, P_{wake} results from the induced drag, D_i and the airspeed, V

$$P_{wake} = D_i\, V \quad . \tag{5.1}$$

The induced drag, D_i is calculated with the equation

$$D_i = \frac{1}{2}\, \rho\, V^2 C_{D_i} S \quad . \tag{5.2}$$

For calculating the induced drag, the drag coefficient, C_{Di} is required

$$C_{D_i} = \frac{C_L^2}{\pi\, A\, e} \quad . \tag{5.3}$$

The lift coefficient, C_L needed for C_{Di} is determined by

$$m\, g = L = \frac{1}{2}\, \rho\ V^2\, C_L\, S \tag{5.4}$$

$$C_L = \frac{2\,m\,g}{\rho\ V^2\,S} \tag{5.5}$$

and can be inserted into the formula for the calculation of the induced drag

$$D_i = \frac{2\ m^2\,g^2}{\pi\ A\ e\ \rho\ V^2\,S}\ . \tag{5.6}$$

The multiplication of the induced drag, D_i with the airspeed, V results the formula for the induced power, P_{wake}

$$P_{wake} = \frac{2\,g^2}{\pi}\ \frac{\frac{m}{S}}{Ae}\ \frac{m}{\rho\ V}\ . \tag{5.7}$$

The formula can be split into three factors. The first factor includes constants, such as the gravitational acceleration, g and π. The second factor involves the individual aircraft design parameters wingload, $\frac{m}{S}$, aspect ratio, A and Oswald factor, e. The third factor consists of parameters, which can be determined from flight operations: aircraft mass, m, approach speed, V and air density, ρ which depends on the airfield altitude.

The aircraft aspect ratio can be written as

$$A = \frac{b^2}{S}\ . \tag{5.8}$$

Inserting the aspect ratio from (5.8) into (5.7) leads another form of the equation for P_{wake}

$$P_{wake} = \frac{2\,g^2}{\pi}\ \frac{1}{b^2 e}\ \frac{m^2}{\rho\ V}\ . \tag{5.9}$$

As shown and explained in Camilo (2022), the induced power can also be derived from the energy of Lamb-Oseen vortices shed from the wing

$$P_{wake} = D_i\,V = E_k\,V\ . \tag{5.10}$$

Here, E_k represents the kinetic energy per unit distance travelled. Since energy or work is defined as force multiplied by distance, dividing energy by distance results in a quantity with the unit of force. When this value, E_k, is multiplied by the flight speed V, it also gives the induced power.

The circulation for an elliptically loaded wing is given by

$$\Gamma_v = \frac{mg}{\rho s_0 b V} \quad . \tag{5.11}$$

Assuming that the vorticity fields of the left and right vortices remain separate, the exact crossflow kinetic energy can be estimated with

$$E_k = \rho \cdot \frac{\Gamma_v^2}{2\pi}\left[\ln\left(\frac{s_0 b}{r_c}\right) + C\right] \tag{5.12}$$

where C is a constant depending on the particular circulation profile. According to Camilo (2022), $C = 0{,}0562$ can be used for the Lamb- Oseen vortices. However, the value of the braced term can be obtained as

$$\frac{(2s_0)^2}{e} \approx \ln\left(\frac{s_0 b}{r_{c,0}}\right) + C \qquad with\ s_0 = \frac{\pi}{4} \quad . \tag{5.13}$$

Substituting (5.13) in (5.12) leads to

$$E_k = \rho \cdot \frac{\Gamma_v^2}{2\pi}\left[\frac{(2s_0)^2}{e}\right] \quad . \tag{5.14}$$

Inserting Γ_v into (5.14) gives us

$$E_k = \rho \cdot \frac{\frac{m^2 g^2}{\rho^2 {s_0}^2 b^2 V^2}}{2\pi}\left[\frac{(2s_0)^2}{e}\right] \tag{5.15}$$

$$E_k = \rho \cdot \frac{m^2 g^2}{\rho^2 {s_0}^2 b^2 V^2\ 2\pi}\frac{4{s_0}^2}{e} \tag{5.16}$$

and finally

$$E_k = \frac{m^2 g^2}{\rho b^2 V^2\ \pi}\frac{2}{e} \quad . \tag{5.17}$$

Multiplying E_k with V, as in (5.10), leads to

$$P_{wake} = E_k\, V \tag{5.18}$$

$$P_{wake} = \frac{m^2 g^2}{\rho b^2 V^2 \pi} \frac{2}{e} V \tag{5.19}$$

and yields induced power, P_{wake} as in (5.9)

$$P_{wake} = \frac{2\, g^2}{\pi} \frac{1}{b^2 e} \frac{m^2}{\rho\ V} \quad . \tag{5.20}$$

To compute the induced power using the equation from the previous section, the Oswald efficiency factor must be included. Nita (2012) presents two methods for estimating this factor, the method used for the calculation is presented in the following section.

5.2 Calculation of the Oswald Factor without Input of $C_{D,0}$

To compute the induced power using the equation from the previous section, the Oswald efficiency factor must be included. Nita (2012) presents two methods for estimating this factor, the method used for the calculation is presented here.

According to Nita (2012), the equation for calculating the Oswald factor without using the zero-lift drag coefficient, $C_{D,0}$ is

$$e = e_{theo} \cdot k_{e,F} \cdot k_{e,D0} \cdot k_{e,M} \cdot k_{e,WL} \quad . \tag{5.21}$$

Where e_{theo} is the theoretical Oswald factor for swept wings

$$e_{theo} = \frac{1}{1 + f(\lambda - \Delta\lambda) \cdot A} \tag{5.22}$$

with

$$\Delta\lambda = -0.357 + 0.45 \cdot e^{-0.0375 \cdot \varphi 25} \tag{5.23}$$

and

$$f(\lambda - \Delta\lambda) = 0.0524(\lambda - \Delta\lambda)^4 - 0.15(\lambda - \Delta\lambda)^3 + 0.1659(\lambda - \Delta\lambda)^2 - 0.0706(\lambda - \Delta\lambda) + 0.0119 \quad . \tag{5.24}$$

Where λ is the taper ratio, A the Aspect ratio and φ_{25} the sweep angle in degrees measured at a quarter of the chord length.

According to Nita (2012) $k_{e,F}$ in the equation for the Oswald factor, e is a correction factor which considers the losses due to the fuselage and is calculated with

$$k_{e,F} = 1 - 2\left(\frac{d_F}{b}\right)^2 \quad . \tag{5.25}$$

Where d_F is the diameter of the fuselage and b the wingspan.

$k_{e,D0}$ is a correction factor in the equation for the Oswald factor, e which considers the viscous drag due to lift and depends on the aircraft category. The $k_{e,D0}$ Correction Factor for Different Aircraft Categories are presented in Table 5.1.

Table 5.1 $ke,D0$ Correction Factor for Different Aircraft Categories Nita (2012)

Aircraft category	ke,D_0
Jet	0,873
Business Jet	0,864
Turboprop	0,804
General Aviation	0,804

$k_{e,M}$ is a correction factor which considers compressibility effects on induced drag and can be calculated with

$$k_{e,M} = a_e \left(\frac{M}{M_{comp}} - 1\right)^{b_e} + c_e \tag{5.26}$$

with the parameters

$$a_e = -0{,}0015 \tag{5.27}$$

$$b_e = 10.82 \tag{5.28}$$

$$c_e = 1 \tag{5.29}$$

$$M_{comp} = 0{,}3 \quad . \tag{5.30}$$

$k_{e,WL}$ is a correction factor for accounting the positiv effects of winglets influencing the Oswald factor, e. The correction factor $k_{e,WL}$ is only used for aircraft with winglets and is calculated with

$$k_{e,WL} = \left(1 + \frac{2}{k_{WL}} \cdot \frac{h}{b}\right)^2 \quad . \tag{5.31}$$

In (5.31) h is the winglet height, b the wingspan and for k_{WL} the average value of 2,83 can be used according to Nita (2012).

5.3 Simplifications Made for the Oswald Factor for Induced Power Calculations

$$e = e_{theo} \cdot k_{e,F} \cdot k_{e,D0} \cdot k_{e,M} \cdot k_{e,WL}$$

As shown in Camilo (2022) in Appendix B, values for e_{theo} and $k_{e,WL}$ were calculated based on individual aircraft parameters, following the methodology described in Nita (2012). Those individually determined values were grouped according to engine type jet or turboprop. Based on this grouping, mean values for e_{theo} were calculated. For piston and turboshaft-powered aircraft, the same average value as for turboprops were applied. This approach results in the following assumptions:

$e_{theo,Jet}$ = 0,9809 for Jets
$e_{theo,Turboprop}$ = 0,9744 for Turboprop and other aircraft
$k_{e,WL}$ =1,0901 for aircraft equipped with winglets

Furthermore, average values are taken from Nita (2012) for $k_{e,F}$ and $k_{e,\mathrm{D0}}$ and are presented in Table 5.2.

Table 5.2 $k_{e,F}$ and $k_{e,\mathrm{D0}}$ Correction Factor for Different Aircraft Categories Nita (2012)

Aircraft category	$k_{e,F}$	$k_{e,\mathrm{D0}}$
Jet	0,973	0,873
Business Jet	0,971	0,864
Turboprop	0,979	0,804
General Aviation	0,971	0,804

$k_{e,M}$ is a correction factor which considers compressibility effects on induced drag. Since this thesis only considers the Mach numbers of aircraft on approach, and they are below the compressibility Mach number, this factor for estimating the Oswald factors is not considered further.

6 Induced Power Results

6.1 Results for the Induced Power Calculation for the FAA ACD

After calculating the induced power for each aircraft model in the FAA Aircraft Characteristics Database, results were obtained for 382 out of 388 aircraft and are presented in Appendix A, Table A.1. For six models, no calculation was possible due to missing approach speed or maximum landing weight data. The range of induced power spans from as low as 0.0067 MW for the Aeronca 7AC to 20.63 MW for the Airbus A380-800.

Based on comparisons with existing wake turbulence classification systems, namely Eurocontrol (2024) and ICAO (2021), the aircraft in the database were also categorized according to their induced power. To achieve the highest possible alignment and comparability with existing classifications, the underlying classification parameters from ICAO and Eurocontrol were applied to all aircraft models in the FAA ACD, and the category boundaries for the HAW WTC were defined accordingly. This leads to the categorization HAWEU based on RECAT EU as shown in Table 6.1 and Figure 6.1.

Table 6.1 HAWEU WTC in Comparison to RECAT-EU

HAWEU WTC	Induced Power [MW]
CAT I	≥ 20
CAT II	≥ 10 – 20
CAT III	≥ 5 – 10
CAT IV	≥ 2 – 5
CAT V	≥ 0.5 – 2
CAT VI	< 0.5

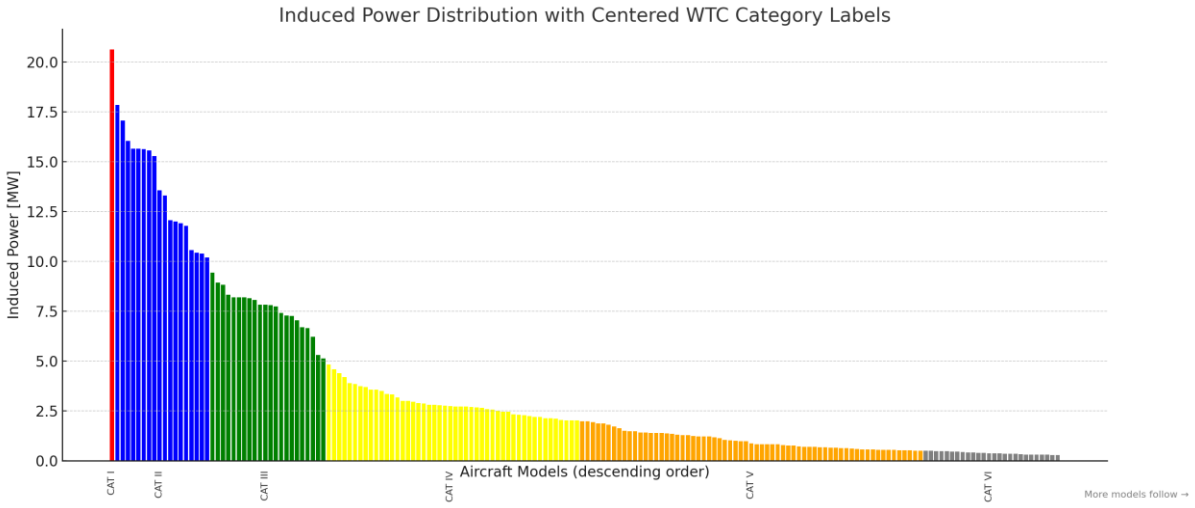

Figure 6.1 HAWEU WTC Based on RECAT-EU

In comparison with the RECAT-EU classification system, which consists of six categories, the distribution of aircraft is as follows: 1 model falls into CAT I, 18 models into CAT II, 22 into CAT III, 48 into CAT IV, 65 into CAT V, and 228 models into CAT VI. Several well-known aircraft models are included in the overview provided in Table 6.2.

Table 6.2 Sample Table for Models and their Categories Based on Induced Power in Comparison to RECAT-EU

CAT I	**CAT II**	**CAT III**	**CAT IV**	**CAT V**	**CAT VI**
>20MW	20-10 MW	10-5MW	5-2 MW	2-0,5 MW	<0,5MW
A380-800	B747-8	A350-1000	A320-Family	Canadair CRJ-900	Cessna Citation
	C17	B787-X	B737-Family	Embraer 170	BAe HS125
	B777-9	A330-800	B717-200	Gulfstream IV	Cessna Excel/ XLS
	A340-600	B767-3	Embraer 190	Embraer 135BJ L600	Embraer Phenom 300
	MD11	B757-3	A220-300		

A second HAW WTC, called HAWICAO, was developed in comparison with the ICAO RECAT classification, following the same methodology as previously described for RECAT-EU. This categorisation classifies all aircraft like the RECAT-ICAO into 7 different categories. The corresponding results are presented in Appendix B.

6.2 Comparison to other Classifications

Using the data provided in the FAA Aircraft Characteristics Database, the induced power was successfully calculated for 382 out of 388 aircraft models. Based on these calculations, each aircraft was assigned a new HAW WTC category.

When comparing this new categorization to existing systems by Eurocontrol (2024) and ICAO (2021), the following deviations were observed and are shown in Appendix C (RECAT-EU) and Appendix D (RECAT-ICAO) in detail:

- HAWEU deviation from RECAT-EU classification: 47 models (12.3%)
- HAWICAO deviation from RECAT-ICAO classification: 56 models (14.6%)
- Deviation from both RECAT-ICAO and RECAT-EU: 31 models (8.1%)

This means that the new HAW_WTC categorization aligns with either RECAT-ICAO or RECAT-EU classifications in 91.9% of the cases. However, a subset of aircraft, presented in Appendix E, is classified differently and does not correspond to either existing system.
These discrepancies can be attributed to the fundamentally different methodologies on which the respective classification systems are based. While the ICAO and EUROCONTROL categorizations primarily rely on structural parameters such as Maximum Takeoff Weight and wingspan, the HAW approach is grounded in a physics-based calculation of induced power

$$P_{wake} = \frac{2\,g^2}{\pi}\,\frac{\frac{m}{S}}{Ae}\,\frac{m}{\rho\,V} \tag{5.7}$$

or with inserting the aspect ratio

$$P_{wake} = \frac{2\,g^2}{\pi}\,\frac{1}{b^2 e}\,\frac{m^2}{\rho\,V}\ . \tag{5.9}$$

Equation (5.7) indicates that the induced power P_{wake} is directly proportional to the aircraft mass, provided that the wing loading $\frac{m}{S}$ and aspect ratio A remain constant. This implies that, for a geometrically scaled aircraft with unchanged aerodynamic characteristics, an increase in mass results in a proportional increase in induced power. In other words, while the aerodynamic efficiency is preserved, the greater lift required to support the higher mass leads to increased energy being transferred into the aircrafts wake.

Equation (5.9) illustrates that induced power increases quadratically with aircraft mass, as a heavier aircraft requires more lift, thereby transferring more energy into the wake. Conversely, as noted by Scholz (2018), induced power decreases with increasing wingspan and higher approach speed.

This flight physics-based approach fundamentally differs from the classifications by ICAO and Eurocontrol, assigning a different category due to the influence of an aircraft wingspan. A larger wingspan enables the aircraft to interact with a greater volume of air, which reduces the required downwash velocity and thus diminishes the wake's energy intensity. The value of induced power therefore serves as a direct measure of the energetic intensity of wake turbulence, and, by extension, the aerodynamic hazard posed to following aircraft. Consequently, the Classifications of ICAO and Eurocontrol are not right in assigning higher wake turbulence categories to aircraft with the same mass but higher wingspan.

Due to this classification difference, aircraft characterized by a given MTOW, relatively small wingspan, and low approach speeds are likely to produce higher wake turbulence and are consequently assigned to higher categories within the HAW system than in conventional classification frameworks. Examples include the C17, DC10, MD11, RJ1H, RJ85, and FA20.

On the other hand, aircraft with a given MTOW but large wingspans and higher approach speeds may be assigned to a lower category in the HAW system. This applies, for instance, to the B787, A350, A340, and A330 families, as well as the P-8 Poseidon, which has a wider wingspan than other B737 variants.

6.3 Induced Power Separation Chart

Based on the newly derived induced power values, a classification (Table 6.1) and corresponding separation chart can be developed, similar to the one used by Eurocontrol, and is presented in Table 6.3.

Table 6.3 HAW WTC Separation Minima Based on RECAT-EU (Eurocontrol 2024)

Leader Follower	CAT I	CAT II	CAT III	CAT IV	CAT V	CAT VI
CAT I	3NM	4NM	5NM	5NM	6NM	8NM
CAT II		3NM	4NM	4NM	5NM	7NM
CAT III			3NM	3NM	4NM	6NM
CAT IV						5NM
CAT V						4NM
CAT VI						3NM

This approach offers an advantage over previous separation charts by allowing individual aircraft parameters to be incorporated into the calculation of induced power, enabling in- flight classification of approaching aircraft into specific categories. However, it still results in fixed category boundaries and does not provide a continuous and seamless separation scheme. Therefore, the following chapter introduces the *Development of a New Approach Separation Model*.

7 Development of a New Approach Separation Model

This section introduces two mathematical models developed to calculate wake turbulence separation minima based on the induced power of aircraft. The objective is to explore a continuous, physics-based approach as an alternative to conventional category-based systems such as those defined by ICAO and Eurocontrol.

To achieve this, two separate classification schemes, HAWEU and HAWICAO, as shown in Chapter 6.1, were derived. Each one is oriented toward the structure of an existing categorization system: one based on the RECAT-EU scheme with six categories, and the other based on RECAT-ICAO with seven categories. For each system, new HAW-induced power categories were defined with boundaries aligned to their respective standards.

To enable modeling and parameter estimation, average values from each induced power category range, presented in Table 6.1 and Table B.1. These average values were used as input for the derivation of separation distances, as used by Eurocontrol and ICAO. Although each model references a different classification system, both are based on the same underlying physical principle, namely, the energy imparted into the wake vortex system, quantified through induced power. This allows for a direct comparison of outcomes across two regulatory frameworks.

7.1 Mathematical Model and Parameter Definition

The required separation distance, d, in nautical miles (NM), between a leading and a following aircraft is calculated using the following general non-linear formula

$$d = n + a\,\Delta P^{u}\,P1^{v}\,P2^{w} \quad . \tag{7.1}$$

- d: Required separation in NM
- ΔP: Difference in induced power (P1 - P2) in megawatts (MW)
- $P1$: Induced power of the leading aircraft (MW)
- $P2$: Induced power of the following aircraft (MW)
- n, a, u, v, w: Empirical model parameters derived through optimization.

Two parameter sets were optimized using the Excel Solver to best fit the separation values defined in the Charts by ICAO (Table 4.1) and RECAT-EU (Figure 4.7) respectively. The optimization was performed using the mean induced power values of each category as input. These mean values were used based on the predefined category boundaries, as outlined in the

respective HAW-induced power classification tables Table 6.1 and Table B.1. The objective with the solver was to minimize the sum of squared errors between model-predicted and official separation values from RECAT ICAO and RECAT EU. The most effective parameter set for the separation formula of each model is presented in Table 7.1.

Table 7.1 Optimized Parameters for the RECAT-EU- and RECAT-ICAO-Based Separation Model

Optimized parameters for the RECAT-EU-based model HAWEU:	Optimized parameters for the RECAT-ICAO-based model HAWICAO:
$n = 2.9661$	$n = 2.6637$
$a = 0.5029$	$a = 0.2900$
$u = 0.2635$	$u = 0.0572$
$v = 0.3351$	$v = 0.7925$
$w = -0.3629$	$w = -0.3853$

While the individual coefficients differ due to the underlying structure of the respective classification systems, both sets reflect the same physical relationships:

- An increasing induced power differential (ΔP) raises the required separation.
- A larger leading aircraft power ($P1$) also increases spacing needs.
- A higher trailing aircraft power ($P2$) typically results in a reduced need for separation, reflecting its greater tolerance to wake energy.

The variations in parameter values reflect the differences in how ICAO and RECAT-EU define their separation requirements. Nevertheless, the models yield similar separation minima when applied to representative data.

The attempt to develop a formula for aircraft separation based on the use of extreme values, instead of the currently used mean values, of each induced-power category, resulted, when applying the Solver, in parameter values that could not be plausibly explained within the framework of the separation principle. Consequently, this methodology was not pursued further, to exemplarily calculate the resulting distances between aircraft based on induced power.

7.2 Resulting Approach Separation Minima

The resulting separation minima examples, presented in Table 7.2, were computed using both sets of model parameters and compared to the official RECAT-ICAO and RECAT-EU reference charts. These values align closely with the respective separation schemes and demonstrate that both approaches, depending on their underlying separation system, lead to comparable operational recommendations when applied through a physics-based model. This

supports the fact that a continuous model can be flexibly adapted to inflight varying aircraft parameters in induced power calculation and offering more separation optimization.

Table 7.2 Resulting Approach Separation Minima

Leader	P1 (MW)	Follower	P2 (MW)	ΔP (MW)	Required Separation (NM)			
					Calculated HAWEU	RECAT-EU	Calculated HAWICAO	RECAT-ICAO
A388	20,63	A388	20,63	0,00	2.97	3	2.66	-
A388	20,63	A320	2,67	17,96	5.04	5	5.24	5
B773	11,92	E195	2,02	9,90	4.6	5	4.46	5
B773	11,92	C56X	0,246	11,674	6.63	7	6.75	7
AT75	0,836	B350	0,176	0,660	3.76	4	3.14	-

8 Summary

Traditional and widely used wake turbulence classification systems, such as RECAT-EU and RECAT-ICAO, rely on generalized groupings based on aircraft characteristics like Maximum Take-Off Weight (MTOW) and wingspan. Based on these groupings and operational experience, standardized approach separation charts were developed to ensure safe sequencing of aircraft and efficient traffic flow in controlled airspace. Over time, these classifications have evolved toward a larger number of finer categories to improve airspace efficiency and reduce errors in aircraft assignments. However, the fixed nature of such categories limits their flexibility in accounting for dynamic aircraft parameters encountered during actual operations, such as aircraft mass, approach speed, and aerodynamic configuration. Moreover, the reliance on simplified indicators like MTOW and wingspan can lead to misclassification of certain aircraft models. In such cases, an aircraft may be assigned a category that is either too conservative, leading to unnecessarily large separation distances, or too low, potentially affecting safety margins.

In contrast, the HAW approach introduces a performance-based, classification system based on continuous parameters that reflect the actual aerodynamic wake impact of each aircraft more accurately. As shown earlier, induced power increases quadratically with aircraft mass, and decreases with greater wingspan and higher approach speed. As a result, aircraft with high mass, relatively short wingspans, and low approach speeds typically generate stronger wake turbulence and are thus placed into higher categories in the HAW classification compared to traditional systems. Conversely, aircraft with relatively high MTOW but larger wingspans and higher approach speeds may be assigned to lower HAW categories than expected under ICAO or RECAT-EU classifications.

These methodological differences naturally result in classification deviations between the systems, which reflect their respective design philosophies. However, such deviations can also reveal untapped optimization potential in specific aircraft models, either by reducing unnecessary separation or by enhancing safety through more appropriate categorization. A closer case-by-case assessment is therefore advisable.

9 Conclusions and Recommendations

It is rather unlikely that existing models exhibit safety deficiencies merely because they assign a smaller separation to certain aircraft than the new formula does. The safe and efficient daily operation at highly frequented airports using the established charts clearly demonstrates this. As already observed, there is a clear trend among aviation authorities toward introducing more categories and finer classifications, but even with six or seven categories, the classification remains rather coarse given the wide variety of aircraft taking off and landing every day. Aircraft models that currently lie at the margins of existing charts may be reclassified in the future, potentially receiving a greater separation from the preceding aircraft as part of a newly created intermediate category. For example, the increase in the separation distance of the Bombardier Challenger 300 on approach behind an Airbus A380 from 7NM to 8NM after re-categorization (ICAO 2021). This also explains why some aircraft are assigned greater separation distances by the developed formula compared to the established charts of ICAO and Eurocontrol. Instead of increasing separation as derived from the formula, another approach could be to correct the entire separation formula downward using a factor, thereby reducing excessive safety margins.

The induced power–based approach to wake turbulence categorization offers a promising alternative to conventional classification systems such as those defined by the ICAO and Eurocontrol. It directly links aircraft parameters to the physical mechanism responsible for wake vortex generation and allows for a more nuanced and continuous classification. Furthermore, the model's flexibility enables the seamless integration of new or modified aircraft types, including those with unconventional configurations, making it suitable for both current fleets and future developments in aviation. The derived formula is particularly suited for implementation in air traffic control systems. Given that all required input parameters are either known or estimable during flight operations, the model could be integrated into ATC decision-making tools. This would allow controllers to assign separation distances individually and dynamically, based on the actual aerodynamic behavior of the aircraft involved.

Even though the formulas for separation minima are based on existing, well established and safe Separation Charts by Eurocontrol and ICAO some influencing factors are still unconsidered and need to be taken into account for future use. In particular, aircraft near category boundaries or those with atypical performance characteristics may require individual assessments. Additionally, the current model includes some simplifications, as described in 5.3, which need to be revised for each aircraft individually. Also, the model does not incorporate the influence of environmental factors and atmospheric conditions influencing the wake turbulence and their behavior. Also, it doesn't reflect the diversity of wake encounter scenarios that trailing aircraft may face in daily operations. Aircraft facing the center of a wake vortex experiences a rolling moment, as mentioned in Camilo (2022), which causes an acceleration in roll. How much an aircraft is affected by this roll acceleration and how do larger aircraft

generate stronger wake vortices need to be considered. This work lays the groundwork, but further research is essential to address remaining uncertainties and operational integration.

List of References

ANDERSON, David, EBERHARDT, Scott, 1999. How Airplanes Fly: A Physical Description of Lift. In: *Sport Aviation*.
Available from: https://bit.ly/3jB3lrE
Archived at: https://perma.cc/TDD7-C24V

BREITSAMTER, Christian, 2010. Wake Vortex Characteristics of Transport Aircraft. In: *Progress in Aerospace Sciences*, vol. 47, no. 2, pp. 89-134.
Available from: https://doi.org/10.1016/j.paerosci.2010.09.002 (Closed Access)

CAMBRIGDE UNIVERSITY PRESS, 2025a. Reclassification. In: *Cambridge Dictionary*.
Available from: https://dictionary.cambridge.org/dictionary/english/reclassification

CAMBRIGDE UNIVERSITY PRESS, 2025b. Separation. In: *Cambridge Dictionary*.
Available from: https://dictionary.cambridge.org/dictionary/english/separation

CAMBRIGDE UNIVERSITY PRESS, 2025c. Use. In: *Cambridge Dictionary*.
Available from: https://dictionary.cambridge.org/dictionary/english/use

CAMBRIGDE UNIVERSITY PRESS, 2025d. FAA. In: *Cambridge Dictionary*.
Available from: https://dictionary.cambridge.org/dictionary/english/faa?q=FAA

CAMILO, Dennis, 2022. Comparing Aircraft Wake Turbulence Categories with Induced Power Calculation. Master Thesis. Hamburg University of Applied Sciences, Aircraft Design and Systems Group (AERO).
Available from: https://nbn-resolving.org/urn:nbn:de:gbv:18302-aero2022-12-30.011

DE KAT, Roeland, 2007. *Vortex Decay behind a Generic Wing-Flap-Jet Aircraft Model: A Time Dependent Vortex Model*. Master Thesis. Delft, The Netherlands: Delft University of Technology.
Available from: https://bit.ly/3FGsd95
Archived at: https://perma.cc/JT35-ESTL

EUROCONTROL 2024. RECAT-EU. European Wake Turbulence Categorisation and Separation Minima on Approach and Departure, Brussels, Belgium: Eurocontrol.
Available from: https://bit.ly/3YIdeWs
Archived at: https://perma.cc/F8R8-9PU8

EWING, Mark, 2025. Wake Turbulence Encounters. ASSURE UAS, Mississippi, USA.
Available from: https://www.assureuas.org/projects/wake-turbulence-encounters/
Archived at: https://perma.cc/GEC6-MWFB

FAA 2021. Consolidated Wake Turbulence, Washington D.C., USA: Federal Aviation Administration.
Available from: https://bit.ly/3ZaWNlC
Archived at: https://perma.cc/RLM4-2DWD

FAA 2025a. Aircraft Characteristics Database, Washington D.C., USA: Federal Aviation Administration.
Available from: http://bit.ly/42mQOuS
Archived at: https://perma.cc/7F5J-XDU7

FAA 2025b. Air Traffic Plans and Publications, Washington D.C., USA: Federal Aviation Administration.
In: *AIM*. Chapter 7. Section 4.
Available from: https://bit.ly/44ALoix
Archived at: https://perma.cc/MDN9-AAE2

ICAO 2021. WAKE TURBULENCE RE-CATEGORISATION, Montreal, Canada: International Civil Aviation Organization.
Available from: https://bit.ly/3GTgl7V
Archived at: https://perma.cc/AC2Y-AVTC

LONGMAN 2025a. Aircraft. In: *Longman Dictionary of Contemporary English*
Available from: https://www.ldoceonline.com/dictionary/aircraft

LONGMAN 2025b. Characteristics. In: *Longman Dictionary of Contemporary English*
Available from: https://www.ldoceonline.com/dictionary/characteristics

LONGMAN 2025c. Database. In: *Longman Dictionary of Contemporary English*
Available from: https://www.ldoceonline.com/dictionary/database

NIŢĂ, Mihaela, SCHOLZ, Dieter, 2012. Estimating the Oswald Factor from Basic Aircraft Geometrical Parameters. In: *Publikationen zum DLRK 2012* (Deutscher Luft- und Raumfahrtkongress, Berlin, 10. - 12. September 2012).
Available from: https://nbn-resolving.org/urn:nbn:de:101:1-201212176728
Archived at: https://perma.cc/TM6M-SEWP

SCHOLZ, Dieter, 2018. Definition and Discussion of the Intrinsic Efficiency of Winglets. In: *INCAS BULLETIN*, vol. 10, 1/2018, pp. 117-134.
Available from: https://doi.org/10.13111/2066-8201.2018.10.1.12
Archived at: https://perma.cc/SJF6-K7AB

SCHOLZ, Dieter, 2022. *Airbus A380 - Ein Nachruf*. Report. Hamburg: Hamburg University of Applied Sciences, Aircraft Design and Systems Group (AERO).
Available from: https://doi.org/10.48441/4427.402
Archived at: https://perma.cc/PE7T-MXMP

SKYBRARY 2025. Wake Vortex Turbulence. In: *Skybrary Aviation Safety*
Available from: https://skybrary.aero/articles/wake-vortex-turbulence
Archived at: https://perma.cc/39UR-B8HE

All online resources have been accessed on 30.06.2025 or later.

Appendix A – Induced Power Calculation

For the calculation of the induced power during approach, the typical values of ρ = 1,225 kg/m³ and g = 9,81 m/s² were used.

Table A.3 Induced Power calculation for each aircraft model

ICAO-CODE	Pwake in MW	MALW in kg	Span, b in m	Vapp in m/s	Oswald factor	ICAO-CODE	Pwake in MW	MALW in kg	Span, b in m	Vapp in m/s	Oswald factor
A10	1,398	22700,2	17,53	72,02	0,8332	**CRJ2**	0,776	20275,8	20,94	72,53	0,8332
A124	15,662	330003,2	73,30	77,67	0,8332	**CRJ7**	1,476	30391,0	23,26	69,44	0,8332
A19N	2,508	62500,7	35,81	66,87	0,9083	**CRJ9**	1,491	33339,4	24,84	72,53	0,8332
A20N	2,767	67400,4	35,81	70,47	0,9083	**CRUZ**	0,015	598,7	8,78	20,06	0,7607
A21N	3,849	79200,8	35,81	69,96	0,9083	**CVLP**	0,497	18053,2	27,98	55,04	0,7607
A306	8,069	137997,8	44,83	70,47	0,8332	**CVLT**	0,640	23587,0	32,09	55,04	0,7670
A30B	7,837	136001,5	44,83	70,47	0,8332	**D328**	0,543	14390,4	20,97	56,58	0,7670
A310	6,701	124000,7	43,89	71,50	0,8332	**DA40**	0,014	1091,8	11,95	39,61	0,7607
A318	2,741	57500,7	34,11	62,24	0,8332	**DA42**	0,023	1700,1	13,56	45,27	0,7607
A319	2,465	61000,6	35,81	64,81	0,9083	**DC10**	12,067	197768,3	50,38	76,65	0,8332
A320	2,673	66000,6	35,81	69,96	0,9083	**DC3**	0,192	11067,8	29,02	49,90	0,7607
A321	3,558	77801,0	35,81	73,05	0,9083	**DC3S**	0,214	11067,8	27,43	49,90	0,7607
A332	7,820	182001,7	60,29	69,96	0,8332	**DC3T**	0,221	11793,5	28,95	48,87	0,7670
A333	8,195	187001,7	60,29	70,47	0,8332	**DC6**	1,477	40007,3	35,81	55,56	0,7607
A337	8,195	186999,9	60,29	70,47	0,8332	**DC87**	5,129	113394,7	45,23	73,56	0,8332
A338	7,039	186002,0	64,00	72,02	0,8332	**DC91**	1,635	37058,9	27,25	67,90	0,8332
A339	7,422	191000,6	64,00	72,02	0,8332	**DC93**	2,204	44906,1	28,44	67,90	0,8332
A342	7,254	181002,0	60,29	74,59	0,8332	**DC95**	2,655	49895,7	28,47	69,44	0,8332
A343	8,162	192002,2	60,29	74,59	0,8332	**DH8A**	0,485	15376,9	25,91	47,33	0,7670
A345	12,011	246002,4	63,46	75,10	0,8332	**DH8B**	0,503	15649,1	25,91	47,33	0,7670
A346	13,301	265002,7	63,46	78,70	0,8332	**DH8C**	0,618	19051,1	27,43	50,93	0,7670
A359	7,815	207002,2	64,75	72,02	0,9083	**DH8D**	0,984	28009,6	28,44	64,30	0,7670
A35K	9,433	233002,4	64,74	75,62	0,9083	**DHC2**	0,063	2313,3	14,63	26,23	0,7607
A388	20,632	394003,9	79,76	70,99	0,8332	**DHC6**	0,136	5579,2	19,81	38,07	0,7670
A400	8,207	123000,1	42,40	66,87	0,7670	**DHC7**	0,690	19051,1	28,35	42,70	0,7670
A5	0,009	684,9	10,61	30,35	0,7607	**DV20**	0,010	729,8	10,88	30,35	0,7607
AA1	0,016	680,4	7,44	35,49	0,7607	**E110**	0,190	5699,9	15,33	47,33	0,7670
AA5	0,020	997,9	9,57	35,49	0,7607	**E120**	0,392	11700,1	19,78	58,13	0,7670
AC11	0,037	1424,3	10,00	36,01	0,7607	**E135**	0,818	18700,0	20,05	63,79	0,8332
AC50	0,028	1950,5	14,93	39,61	0,7607	**E145**	0,818	18700,0	20,05	63,79	0,8332
AC56	0,022	1950,5	14,93	49,90	0,7607	**E170**	1,416	33299,9	26,00	63,79	0,9083
AC68	0,086	3855,6	15,09	49,90	0,7607	**E190**	1,936	43000,5	28,71	63,79	0,9083
AC6L	0,120	4082,4	13,44	50,41	0,7607	**E195**	2,018	45800,6	28,71	69,44	0,9083
AC80	0,096	3855,6	14,23	49,90	0,7670	**E290**	1,976	49050,2	33,71	64,30	0,8332
AC90	0,100	4388,6	15,88	49,90	0,7670	**E295**	2,029	54000,3	35,11	69,96	0,8332
AC95	0,097	4388,6	15,88	51,44	0,7670	**E35L**	0,664	18500,0	21,09	63,79	0,9083
AEST	0,079	2721,6	11,19	49,38	0,7607	**E45X**	0,864	20000,0	19,99	63,79	0,9083
AN12	2,321	58000,5	38,04	65,33	0,7670	**E50P**	0,152	4429,8	12,28	51,44	0,8332
AN72	1,250	33000,5	31,88	51,44	0,8332	**E545**	0,512	14750,1	20,24	57,10	0,9083
AR11	0,007	567,0	10,97	25,21	0,7607	**E550**	0,565	15660,0	20,27	58,13	0,9083
ASTR	0,332	9389,5	16,06	61,73	0,8332	**E55P**	0,209	7568,3	15,91	59,67	0,9083
AT3T	0,071	3175,2	15,57	38,07	0,7670	**E75L**	1,022	34000,3	31,00	64,81	0,9083
AT43	0,542	16402,1	24,60	53,50	0,7670	**E75S**	1,211	34000,3	28,71	63,79	0,9083
AT44	0,542	16400,3	24,60	53,50	0,7670	**EA50**	0,060	2456,2	11,37	46,81	0,8332
AT45	0,675	18300,4	24,60	53,50	0,7670	**ERCO**	0,009	571,5	9,14	28,29	0,7607
AT46	0,675	18300,4	24,60	53,50	0,7670	**EVOT**	0,046	1905,1	11,28	40,64	0,7670
AT5T	0,086	3628,8	15,85	39,61	0,7670	**F15**	4,821	36740,4	13,04	98,77	0,8332

AT6T	0,140	5443,2	17,07	47,33	0,7670	**F16**	2,703	19187,2	9,97	82,30	0,8332
AT72	0,692	21349,9	27,06	58,64	0,7670	**F18H**	3,706	25401,4	12,31	68,93	0,8332
AT73	0,725	21349,9	27,03	56,07	0,7670	**F18S**	4,205	29937,4	13,62	68,93	0,8332
AT75	0,836	21850,2	24,57	61,73	0,7670	**F22**	#WERT!	0,0	13,56	74,59	0,8332
AT76	0,767	22350,1	27,03	58,13	0,7670	**F2TH**	0,764	17826,4	19,32	66,87	0,8332
AT8T	0,198	7257,6	18,07	52,98	0,7670	**F406**	0,097	4246,1	15,09	52,98	0,7670
B18T	0,138	4309,2	14,02	44,75	0,7670	**F900**	0,979	20185,1	19,32	66,87	0,8332
B190	0,177	7257,6	17,68	62,24	0,7670	**FA10**	0,408	8001,5	13,08	55,04	0,8332
B2	#WERT!	0,0	52,42	72,02	0,8332	**FA20**	0,630	12392,3	16,31	55,04	0,8332
B350	0,176	6804,0	17,65	55,04	0,7670	**FA50**	0,694	16200,2	18,87	63,79	0,8332
B36T	0,046	1655,6	10,21	37,55	0,7607	**FA7X**	1,308	28304,5	26,21	53,50	0,8332
B37M	2,723	66043,7	35,90	74,59	0,8332	**FA8X**	1,275	28304,5	26,30	54,53	0,8332
B38M	2,999	69309,6	35,90	74,59	0,8332	**FDCT**	0,012	598,7	8,56	26,23	0,7607
B39M	3,335	74344,6	35,90	77,16	0,8332	**G150**	0,303	9843,1	16,95	66,87	0,8332
B461	1,719	35153,8	26,33	62,24	0,8332	**G164**	0,074	2755,6	12,89	40,64	0,7607
B462	1,862	36741,4	26,33	62,76	0,8332	**G280**	0,557	14832,6	19,20	64,30	0,8332
B52	#WERT!	0,0	56,39	72,53	0,8332	**GA5C**	0,998	29189,0	26,32	67,90	0,9083
B703	4,390	97523,4	44,44	65,84	0,8332	**GA6C**	1,222	34836,3	28,70	66,36	0,9083
B712	2,136	45359,7	28,44	71,50	0,8332	**GA7**	0,037	1723,7	11,22	42,18	0,7607
B721	3,502	63503,6	32,92	63,79	0,8332	**GALX**	0,530	13607,9	17,71	66,87	0,8332
B722	3,357	68039,6	33,31	68,42	0,9083	**GC1**	0,027	895,9	8,93	24,69	0,7607
B732	2,457	46720,5	28,35	66,36	0,8332	**GL5T**	1,412	35652,7	28,65	65,84	0,8332
B733	2,246	52526,5	31,21	69,44	0,9083	**GL7T**	1,399	38918,2	31,79	64,30	0,8332
B734	3,166	56110,0	28,89	71,50	0,8332	**GLEX**	1,379	35652,7	28,65	67,39	0,8332
B735	2,718	49895,7	28,89	65,84	0,8332	**GLF2**	1,344	26535,4	20,97	71,50	0,8332
B736	2,031	55112,0	35,78	64,30	0,9083	**GLF3**	1,044	26535,4	23,71	72,02	0,8332
B737	2,805	66043,7	35,78	66,87	0,9083	**GLF4**	1,292	29937,4	23,71	74,07	0,8332
B738	2,556	66349,9	35,78	74,07	0,9083	**GLF5**	1,131	34155,9	28,50	69,96	0,9083
B739	2,860	71400,6	35,78	76,65	0,9083	**GLF6**	1,214	37875,4	30,39	70,47	0,9083
B741	16,037	265354,3	59,65	74,07	0,8332	**H25A**	0,455	10000,0	14,32	64,30	0,8332
B742	17,855	285766,1	59,65	77,16	0,8332	**H25B**	0,389	10591,5	15,67	70,47	0,8332
B743	15,657	260364,7	59,65	73,05	0,8332	**H25C**	0,463	11339,9	15,67	67,90	0,8332
B744	17,059	285766,1	59,65	80,76	0,8332	**HA4T**	0,593	15195,5	18,84	65,84	0,8332
B748	15,279	312074,8	68,39	81,79	0,8332	**HAWK**	0,184	4648,9	9,94	71,50	0,8332
B752	3,734	89812,2	41,09	70,47	0,9083	**HDJT**	0,142	4472,0	12,16	57,10	0,8332
B753	4,578	101605,7	41,09	73,56	0,9083	**HUSK**	0,015	907,2	10,82	30,86	0,7607
B762	5,311	117935,2	47,58	69,44	0,8332	**IL76**	8,941	152500,2	50,50	61,21	0,8332
B763	6,218	145151,0	50,90	72,02	0,9083	**J328**	0,478	14390,4	20,97	59,16	0,8332
B764	7,277	158759,0	51,90	77,16	0,8332	**JS31**	0,191	6599,8	15,85	59,16	0,7670
B772	10,205	213190,6	60,93	72,02	0,8332	**JS32**	0,232	7080,2	15,85	56,07	0,7670
B773	11,918	237684,8	60,93	76,65	0,8332	**JS41**	0,292	10115,2	18,41	67,39	0,7670
B778	10,573	266261,5	71,75	78,19	0,8332	**K35R**	7,731	119232,1	39,87	69,44	0,8332
B779	10,435	266261,5	71,75	79,22	0,8332	**KODI**	0,100	3290,8	13,72	37,55	0,7670
B77L	13,567	260818,3	64,64	72,02	0,8332	**L29B**	1,171	16329,5	16,55	49,90	0,8332
B7W	11,778	251292,8	64,80	76,65	0,8332	**L5**	0,018	929,9	10,36	29,84	0,7607
B788	6,657	172366,9	60,13	74,07	0,8332	**L8**	0,010	635,0	10,67	23,66	0,7607
B789	8,328	192778,7	60,13	74,07	0,8332	**LA4**	0,028	1220,2	11,58	26,23	0,7607
B78X	8,823	201850,7	60,13	76,65	0,8332	**LJ23**	0,225	5388,7	10,85	65,84	0,8332
BA11	1,878	39462,5	26,97	68,42	0,8332	**LJ24**	0,225	5388,7	10,85	65,84	0,8332
BCS1	2,143	54200,3	35,08	66,87	0,8332	**LJ25**	0,233	5669,5	10,85	70,47	0,8332
BCS3	2,579	60600,6	35,08	69,44	0,8332	**LJ31**	0,263	6940,0	13,35	61,73	0,8332
BE10	0,151	5084,8	13,99	57,10	0,7670	**LJ35**	0,265	6486,4	12,04	65,84	0,8332
BE18	0,116	4263,8	15,15	44,75	0,7607	**LJ40**	0,339	8709,1	14,57	63,27	0,8332
BE19	0,016	906,7	10,00	33,44	0,7607	**LJ45**	0,339	8709,1	14,57	63,27	0,8332
BE20	0,138	5670,0	16,61	55,04	0,7670	**LJ55**	0,311	7711,1	13,35	64,30	0,8332
BE23	0,023	1111,3	10,00	36,01	0,7607	**LJ60**	0,410	8845,1	13,35	64,30	0,8332
BE24	0,026	1247,4	10,00	40,12	0,7607	**LJ70**	0,294	8709,1	15,51	64,30	0,8332
BE30	0,153	6350,4	17,65	55,04	0,7670	**LJ75**	0,294	8709,1	15,51	64,30	0,8332
BE33	0,042	1542,2	10,21	35,49	0,7607	**LNC4**	0,030	1360,8	9,94	41,67	0,7607
BE35	0,036	1542,2	10,82	37,04	0,7607	**LNP4**	0,047	1723,7	9,94	41,67	0,7670

BE36	0,044	1655,6	10,21	39,61	0,7607	**M20P**	0,029	1451,5	11,00	39,61	0,7607
BE40	0,295	7121,5	13,26	58,64	0,8332	**M20T**	0,029	1451,5	11,00	39,61	0,7607
BE50	0,069	2859,9	13,81	41,15	0,7607	**M5**	0,037	1043,3	9,39	22,12	0,7607
BE55	0,054	2313,3	11,52	48,87	0,7607	**MD11**	10,404	195046,7	51,97	81,28	0,8332
BE58	0,061	2449,4	11,52	48,87	0,7607	**MD81**	2,714	58060,4	32,89	68,93	0,8332
BE60	0,086	3073,1	11,98	50,41	0,7607	**MD82**	2,779	58967,6	32,89	69,44	0,8332
BE65	0,087	3492,7	13,99	47,33	0,7607	**MD83**	3,000	63276,8	32,89	74,07	0,8332
BE70	0,082	3719,5	15,33	47,33	0,7607	**MD87**	2,800	58967,6	32,89	68,93	0,8332
BE76	0,039	1769,0	11,58	39,09	0,7607	**MD88**	2,886	58967,6	32,89	66,87	0,8332
BE77	0,014	759,8	9,14	32,41	0,7607	**MD90**	2,955	62142,8	32,89	72,53	0,8332
BE80	0,078	3628,8	15,33	47,33	0,7607	**MU2**	0,212	5000,9	11,95	54,01	0,7670
BE95	0,044	1905,1	11,52	40,64	0,7607	**MU30**	0,202	5987,5	13,26	60,70	0,8332
BE99	0,159	5125,6	13,99	55,04	0,7670	**NAVI**	0,037	1292,8	10,18	28,81	0,7607
BE9L	0,102	4354,5	15,33	51,44	0,7670	**P180**	0,145	5216,4	14,02	62,24	0,7670
BE9T	0,105	4966,9	16,61	55,56	0,7670	**P210**	0,036	1723,7	11,83	38,58	0,7607
BL17	0,034	1508,2	10,42	40,64	0,7607	**P28A**	0,015	966,2	10,67	36,01	0,7607
BL8	0,018	975,2	11,03	28,81	0,7607	**P28B**	0,034	1360,8	10,67	31,89	0,7607
BLCF	15,623	295745,3	64,92	79,73	0,8332	**P28R**	0,026	1315,4	10,79	37,55	0,7607
BT36	0,040	1746,3	11,52	37,55	0,7607	**P28T**	0,023	1247,4	10,79	37,55	0,7607
C120	0,011	680,4	10,15	26,75	0,7607	**P3**	2,275	47119,7	30,39	68,93	0,7670
C130	2,306	58967,6	40,41	60,19	0,7670	**P32R**	0,035	1632,9	11,03	41,15	0,7607
C140	0,011	680,4	10,15	26,75	0,7607	**P32T**	0,035	1632,9	11,03	41,15	0,7607
C150	0,012	725,8	10,12	28,29	0,7607	**P46T**	0,048	2199,9	13,11	38,58	0,7670
C152	0,013	759,8	10,12	28,81	0,7607	**P51**	0,268	5488,5	11,28	58,13	0,7607
C160	1,401	46999,5	39,99	64,30	0,7670	**P68**	0,043	1890,1	12,01	37,55	0,7607
C162	0,011	598,7	9,14	26,23	0,7607	**P750**	0,112	3231,9	12,80	37,04	0,7670
C17	15,569	202721,6	51,75	59,16	0,8332	**P8**	1,976	65771,6	37,67	92,59	0,8332
C170	0,018	997,9	10,97	30,35	0,7607	**PA11**	0,007	553,4	10,82	23,66	0,7607
C172	0,021	1111,3	11,00	31,89	0,7607	**PA12**	0,012	793,8	10,82	28,81	0,7607
C175	0,023	1111,3	11,03	28,81	0,7607	**PA16**	0,016	748,4	8,93	28,81	0,7607
C177	0,027	1134,0	10,82	26,75	0,7607	**PA18**	0,014	793,8	10,76	24,69	0,7607
C180	0,027	1270,1	10,91	32,92	0,7607	**PA20**	0,023	884,5	8,93	28,29	0,7607
C182	0,029	1338,1	10,97	33,44	0,7607	**PA22**	0,024	907,2	8,93	28,81	0,7607
C185	0,039	1519,6	10,91	32,92	0,7607	**PA23**	0,055	2177,3	11,34	43,72	0,7607
C188	0,027	1496,9	12,71	33,95	0,7607	**PA24**	0,024	1315,4	10,97	38,58	0,7607
C195	0,047	1519,6	11,03	26,75	0,7607	**PA25**	0,026	1315,4	11,03	35,49	0,7607
C206	0,040	1632,9	10,97	36,01	0,7607	**PA27**	0,055	2240,8	11,34	46,81	0,7607
C207	0,040	1632,9	11,00	36,52	0,7607	**PA30**	0,036	1632,9	11,22	39,09	0,7607
C208	0,080	3538,1	15,88	40,64	0,7670	**PA31**	0,076	2948,4	12,40	48,87	0,7607
C210	0,036	1723,7	11,22	43,72	0,7607	**PA32**	0,036	1632,9	11,03	40,12	0,7607
C212	0,285	8099,9	18,99	41,67	0,7670	**PA34**	0,047	2047,1	11,86	41,67	0,7607
C240	0,033	1551,3	11,00	40,12	0,7607	**PA36**	0,080	2177,3	11,83	27,78	0,7607
C25A	0,121	5227,7	15,18	58,64	0,8332	**PA38**	0,011	757,5	10,36	30,86	0,7607
C25B	0,137	5783,4	16,25	55,56	0,8332	**PA44**	0,042	1723,7	11,76	33,95	0,7607
C25C	0,221	7103,3	15,48	57,10	0,8332	**PA46**	0,031	1769,0	13,11	38,58	0,7607
C25M	0,113	4490,6	14,42	51,44	0,8332	**PAT4**	0,125	4082,4	13,01	51,44	0,7670
C303	0,027	1635,2	11,89	46,30	0,7607	**PAY1**	0,128	3946,3	13,01	47,33	0,7607
C30J	2,108	58967,6	40,41	65,84	0,7670	**PAY2**	0,126	4082,4	13,01	51,44	0,7607
C310	0,072	2494,8	11,25	44,75	0,7607	**PAY3**	0,117	4685,7	14,54	58,13	0,7670
C320	0,069	2154,6	11,25	34,98	0,7607	**PAY4**	0,139	5034,9	14,54	56,07	0,7670
C335	0,076	2717,0	11,61	47,33	0,7607	**PC12**	0,105	4500,1	16,25	43,72	0,8361
C340	0,074	2717,0	11,61	48,35	0,7607	**PC24**	0,222	7665,8	17,01	55,04	0,8332
C402	0,082	3107,1	13,47	42,70	0,7607	**PRM1**	0,146	5261,7	13,56	61,73	0,8332
C404	0,090	3674,1	14,11	49,38	0,7607	**R721**	3,571	64637,6	32,92	64,81	0,8332
C414	0,069	3061,8	13,47	48,87	0,7607	**R722**	3,889	70080,7	32,92	69,96	0,8332
C421	0,078	3265,9	13,47	49,38	0,7607	**RJ1H**	2,205	40143,3	26,33	63,27	0,8332
C425	0,094	3628,8	13,47	50,41	0,7670	**RJ85**	2,050	38555,7	26,33	62,76	0,8332
C441	0,103	4245,7	15,03	50,41	0,7670	**RV12**	0,013	598,7	8,17	27,26	0,7607
C500	0,140	5148,3	14,36	55,04	0,8332	**S108**	0,020	1088,6	10,33	36,01	0,7607
C501	0,140	5148,3	14,36	55,04	0,8332	**S22T**	0,032	1632,9	11,67	39,61	0,7607

C510	0,084	3628,8	13,17	54,01	0,8332	**SB20**	0,819	21999,9	24,78	62,76	0,7670
C525	0,107	4490,6	14,29	55,56	0,8332	**SBR1**	0,314	7937,9	13,62	64,81	0,8332
C526	0,108	4490,6	14,26	55,04	0,8332	**SBR2**	0,534	10430,0	13,62	65,84	0,8332
C550	0,168	6123,6	15,76	54,01	0,8332	**SC7**	0,114	5670,0	19,78	46,81	0,7670
C551	0,139	5443,2	15,76	51,44	0,8332	**SF34**	0,301	12337,8	22,74	63,79	0,7670
C55B	0,148	6123,6	15,91	60,19	0,8332	**SF50**	0,071	2721,6	11,80	44,75	0,8332
C560	0,198	6894,7	16,49	52,98	0,8332	**SH33**	0,268	10249,9	22,77	49,38	0,7670
C56X	0,246	8482,3	17,16	59,67	0,8332	**SH36**	0,339	12019,9	22,80	53,50	0,7670
C650	0,207	7711,1	16,31	64,81	0,8332	**SR20**	0,022	1315,4	11,67	38,07	0,7607
C680	0,441	12292,5	19,23	55,56	0,8332	**SR22**	0,029	1542,2	11,67	40,12	0,7607
C68A	0,376	12507,9	22,04	51,44	0,8332	**SU95**	1,813	41000,6	27,80	72,02	0,8332
C700	0,505	15195,5	21,00	62,24	0,8332	**SW3**	0,195	5670,0	14,11	54,01	0,7670
C72R	0,021	1111,3	11,00	31,89	0,7607	**SW4**	0,190	7110,1	17,37	57,61	0,7670
C750	0,493	14424,4	19,38	67,39	0,8332	**T210**	0,037	1723,7	11,83	37,55	0,7607
C77R	0,027	1270,1	10,82	33,44	0,7607	**T28**	0,173	3542,1	12,22	31,89	0,7607
C82R	0,030	1338,1	10,97	32,92	0,7607	**T34P**	0,103	2404,1	10,15	35,49	0,7670
CH7A	0,007	553,4	10,21	28,81	0,7607	**T38**	0,369	5485,3	7,71	82,30	0,8332
CH7B	0,015	816,5	10,21	28,81	0,7607	**T6**	0,081	2417,2	12,80	28,81	0,7607
CL30	0,574	15308,9	19,45	64,81	0,8332	**TAYB**	0,010	680,4	10,97	25,72	0,7607
CL35	0,512	15490,3	21,00	63,79	0,8332	**TB20**	0,033	1397,1	9,97	38,58	0,7607
CL41	#WERT!	3532,2	11,12	#WERT!	0,8332	**TBM7**	0,086	2835,0	12,68	38,07	0,7670
CL60	0,659	17236,7	19,60	70,47	0,8332	**TBM8**	0,094	3186,1	12,68	43,72	0,7670
CN35	0,471	16500,0	25,82	56,58	0,7670	**TBM9**	0,092	3186,1	12,83	43,72	0,7670
COL3	0,029	1465,1	11,00	40,12	0,7607	**TEX2**	0,116	3129,8	10,18	52,98	0,7670
COL4	0,029	1465,1	11,00	40,12	0,7607	**TOBA**	0,026	1147,6	10,00	33,44	0,7607
COUR	#WERT!	1542,2	11,89	#WERT!	0,7607	**V22**	#NV	27442,6	13,96	#WERT!	0,7670
CRJ1	0,836	21319,1	21,21	72,53	0,8332	**WW24**	0,360	8618,3	13,65	66,36	0,8332

Appendix B – HAWICAO WTC

Table B.1 Induced Power classification HAWICAO based on RECAT-ICAO

HAWICAO WTC	Induced Power [MW]
CAT I	≥ 20
CAT II	≥ 10 – 20
CAT III	≥ 5 – 10
CAT IV	≥ 2,5 – 5
CAT V	≥ 1,5 – 2,5
CAT VI	≥ 0,75 – 1,5
CAT VII	< 0,75

Table B.2 Examples for each HAWICAO WTC

CAT I >20MW	**CAT II** 20-10 MW	**CAT III** 10-5MW	**CAT IV** 5-2,5 MW	**CAT V** 2,5-1,5 MW	**CAT VI** 1,5-0,75 MW	**CAT VII** <0,75MW
A380-800	B747-8	A350-1000	A320	A319	Canadair CRJ-900	Canadair Challenger 600
	C17	B787-X	B737-8	A220-100	Canadair CRJ-200	Cessna Citation
	B777-9	A330-800	B717-200	Embraer 190	Embraer 170	BAe HS125
	A340-600	B767-3	B737-9	P-8 Poseidon	Embraer 175	Cessna Excel/ XLS
	MD11	B757-3	A321	B717-200	Embraer 145	Embraer Phenom 300

Appendix C – HAWEU Deviation from RECAT-EU

Table C.1 HAWEU & RECAT EU Categories

	Super	Upper heavy	Lower heavy	Upper medium	Lower medium	Light
HAW_CAT	CAT I	CAT II	CAT III	CAT VI	CAT V	CAT VI
EU	A	B	C	D	E	F

Table C.2 HAWEU Deviation from RECAT-EU

ICAO Code	EU	HAWEU	ICAO Code	EU	HAWEU
A124	A	CAT II	F15	E	CAT IV
MD11	C	CAT II	P8	D	CAT V
DC10	C	CAT II	FA20	F	CAT V
C17	C	CAT II	SBR2	F	CAT V
A338	B	CAT III	DC6	D	CAT V
A339	B	CAT III	D328	F	CAT V
A342	B	CAT III	CVLT	D	CAT V
A343	B	CAT III	C160	D	CAT V
A359	B	CAT III	E290	D	CAT V
A35K	B	CAT III	DH8A	E	CAT VI
B78X	B	CAT III	J328	E	CAT VI
B789	B	CAT III	CVLP	E	CAT VI
B788	B	CAT III	CN35	E	CAT VI
A337	B	CAT III	C750	E	CAT VI
A333	B	CAT III			
A332	B	CAT III			
P3	E	CAT IV			
DC93	E	CAT IV			
DC95	E	CAT IV			
RJ85	E	CAT IV			
E195	E	CAT IV			
F18S	E	CAT IV			
F18H	E	CAT IV			
B753	C	CAT IV			
F16	E	CAT IV			
B752	C	CAT IV			
B735	E	CAT IV			
B734	E	CAT IV			
B733	E	CAT IV			
B732	E	CAT IV			
B712	E	CAT IV			
B703	C	CAT IV			
RJ1H	E	CAT IV			

Appendix D –
HAWICAO Deviation from RECAT-ICAO

Table D.1 HAWICAO & RECAT-ICAO Categories

	Super	Upper heavy	Lower heavy	Upper medium	Lower medium	Upper Light	Lower Light
HAW_CAT	CAT I	CAT II	CAT III	CAT VI	CAT V	CAT VI	CAT VII
ICAO	A	B	C	D	E	F	G

Table D.2 HAWICAO Deviation from RECAT-ICAO

ICAO Code	ICAO	HAWICAO	ICAO Code	ICAO	HAWICAO
C17	C	CAT II	AN12	D	CAT V
MD11	C	CAT II	B461	F	CAT V
DC10	C	CAT II	B462	F	CAT V
B788	B	CAT III	B736	D	CAT V
B789	B	CAT III	BA11	F	CAT V
B78X	B	CAT III	RJ85	F	CAT V
A35K	B	CAT III	BCS1	D	CAT V
A359	B	CAT III	AN72	E	CAT VI
A342	B	CAT III	GLF6	E	CAT VI
A339	B	CAT III	GLF5	E	CAT VI
A338	B	CAT III	GLEX	E	CAT VI
A337	B	CAT III	GL7T	E	CAT VI
A333	B	CAT III	GL5T	E	CAT VI
A332	B	CAT III	GA6C	E	CAT VI
A343	B	CAT III	DC6	D	CAT VI
B735	E	CAT IV	E75S	E	CAT VI
DC95	E	CAT IV	C160	D	CAT VI
B734	E	CAT IV	E75L	E	CAT VI
F16	F	CAT IV	DH8D	E	CAT VI
F15	F	CAT IV	AT72	F	CAT VII
F18H	F	CAT IV	E35L	F	CAT VII
F18S	F	CAT IV	CVLT	D	CAT VII
B703	C	CAT IV	DHC7	E	CAT VII
E290	D	CAT V	DH8C	E	CAT VII
E295	D	CAT V	CL60	F	CAT VII
RJ1H	F	CAT V	CVLP	E	CAT VII
DC91	F	CAT V	AT73	F	CAT VII
P8	D	CAT V			
A319	D	CAT V			
C30J	D	CAT V			
C130	D	CAT V			

Appendix E –
Deviation from RECAT-ICAO and RECAT-EU

Table E.1 Deviation from RECAT-ICAO and RECAT-EU

ICAO Code	EU	HAWEU	ICAO	HAWICAO
A332	B	CAT III	B	CAT III
A333	B	CAT III	B	CAT III
A337	B	CAT III	B	CAT III
A338	B	CAT III	B	CAT III
A339	B	CAT III	B	CAT III
A342	B	CAT III	B	CAT III
A343	B	CAT III	B	CAT III
A359	B	CAT III	B	CAT III
A35K	B	CAT III	B	CAT III
B703	C	CAT IV	C	CAT IV
B734	E	CAT IV	E	CAT IV
B735	E	CAT IV	E	CAT IV
B788	B	CAT III	B	CAT III
B789	B	CAT III	B	CAT III
B78X	B	CAT III	B	CAT III
C160	D	CAT V	D	CAT VI
C17	C	CAT II	C	CAT II
CVLP	E	CAT VI	E	CAT VII
CVLT	D	CAT V	D	CAT VII
DC10	C	CAT II	C	CAT II
DC6	D	CAT V	D	CAT VI
DC95	E	CAT IV	E	CAT IV
E290	D	CAT V	D	CAT V
F15	E	CAT IV	F	CAT IV
F16	E	CAT IV	F	CAT IV
F18H	E	CAT IV	F	CAT IV
F18S	E	CAT IV	F	CAT IV
MD11	C	CAT II	C	CAT II
P8	D	CAT V	D	CAT V
RJ1H	E	CAT IV	F	CAT V
RJ85	E	CAT IV	F	CAT V